

# Warming-driven erosion and sediment transport in cold regions

Ting Zhang ®¹, Dongfeng Li ®¹⊠, Amy E. East², Desmond E. Walling³, Stuart Lane ®⁴, Irina Overeem ®⁵, Achim A. Beylich⁶, Michèle Koppes⁵ & Xixi Lu ®¹

#### **Abstract**

Rapid atmospheric warming since the mid-twentieth century has increased temperature-dependent erosion and sediment-transport processes in cold environments, affecting food, energy and water security. In this Review, we summarize landscape changes in cold environments and provide a global inventory of increases in erosion and sediment yield driven by cryosphere degradation. Anthropogenic climate change, deglaciation, and thermokarst disturbances are causing increased sediment mobilization and transport processes in glacierized and periglacierized basins. With continuous cryosphere degradation, sediment transport will continue to increase until reaching a maximum (peak sediment). Thereafter, transport is likely to shift from a temperature-dependent regime toward a rainfalldependent regime roughly between 2100-2200. The timing of the regime shift would be regulated by changes in meltwater, erosive rainfall and landscape erodibility, and complicated by geomorphic feedbacks and connectivity. Further progress in integrating multisource sediment observations, developing physics-based sediment-transport models, and enhancing interdisciplinary and international scientific collaboration is needed to predict sediment dynamics in a warming world.

#### **Sections**

Introduction

Ongoing cryosphere degradation

Changing dynamics of sediment transport

Observed increases in sediment fluxes

Projections and peak sediment

Challenges and complexity

Summary and future perspectives

<sup>1</sup>Department of Geography, National University of Singapore, Singapore, Singapore. <sup>2</sup>US Geological Survey Pacific Coastal and Marine Science Center, Santa Cruz, CA, USA. <sup>3</sup>Department of Geography, College of Life and Environmental Sciences, University of Exeter, Exeter, UK. <sup>4</sup>Institute of Earth Surface Dynamics, University of Lausanne, Lausanne, Switzerland. <sup>5</sup>CSDMS, Institute of Arctic and Alpine Research, University of Colorado Boulder, Boulder, CO, USA. <sup>6</sup>Geomorphological Field Laboratory (GFL), Selbustrand, Norway. <sup>7</sup>Department of Geography, University of British Columbia, Vancouver, Canada. ⊠e-mail: dongfeng@u.nus.edu

#### **Key points**

- A global inventory of cryosphere-degradation-driven increases in erosion and sediment yield is presented, with 76 locations from the high Arctic, European mountains, High Mountain Asia and Andes, and 18 Arctic permafrost-coastal sites.
- Sediment mobilization from glacierized basins is dominated by glacial and paraglacial erosion; transport efficiency is controlled by glaciohydrology and modulated by subglacial, proglacial and supraglacial storage and release, but is interrupted by glacial lakes and moraines.
- Degraded permafrost mainly mobilizes sediment by eroding thermokarst landscapes in high-latitude terrain and unstable rocky slopes in high-altitude terrain, which is sustained by exposing and melting ground ice and sufficient water supply; transport efficiency is enhanced by hillslope-channel connectivity.
- The sediment-transport regime will shift in three stages, from a thermal-controlled regime to one jointly controlled by thermal and pluvial processes, and finally to a regime controlled by pluvial processes.
- Peak sediment yield will be reached with or after peak meltwater.
- Between the 1950s and 2010s, sediment fluxes have increased twoto eight-fold in many cold regions, and coastal erosion rates have more than doubled along many parts of Arctic permafrost coastlines.

#### Introduction

Atmospheric warming is driving rapid cryosphere degradation, with increases in temperature-dependent erosion and sediment-transport processes in the world's high-altitude and high-latitude cold regions<sup>1,2</sup>. There have been substantial increases in fluvial sediment fluxes from the high Arctic, European mountains, high mountain Asia (HMA) and the Andes since the 1950s. These hydrogeomorphic changes are greatly altering terrestrial and coastal landscape evolution, including river and basin reorganization, coastal erosion and delta progradation<sup>3-5</sup>.

Changes in sediment availability and transport capacity<sup>6–8</sup>, mobilization<sup>9</sup> and delivery mechanisms have arisen from cryosphere degradation. For instance, enhanced glacier melt increases meltwater discharge and the amplitude of diurnal discharge variations<sup>10</sup>, increasing fluvial sediment-transport capacity until peak meltwater<sup>11</sup> is reached. Expanded erodible area and enhanced sediment accessibility<sup>12,13</sup> with melt and thaw drive increased sediment availability. Glacier retreat aids sediment mobilization<sup>14</sup>, subglacial sediment export<sup>12,15</sup>, and mass wasting along deglaciated valley walls; increased climate-driven landslide occurrence is already evident in some cold regions<sup>16,17</sup>. Cryosphere degradation is likely to cause a shift from a temperature-dependent sediment-transport regime<sup>8,13,18</sup>, which has existed throughout much of the Holocene into the twentieth century, to a more exclusively rainfall-dependent regime, with sediment transport dominated by rainfall-triggered mass movements<sup>19,20</sup>.

Sediment-transport regime shifts and flux changes will have wide-reaching consequences, with some evidence of these impacts already seen. There are concerns about the impacts on water quality  $^{21}$ , reservoir

sedimentation<sup>10,22,23</sup>, ecological stability<sup>24,25</sup> and water-food-energy security for nearly 2 billion people living in or downstream of mountain areas<sup>21,26,27</sup>. Land-ocean biogeochemical fluxes<sup>19,28-30</sup> and contaminant transport from cryospheric basins will also change. For example, increased sediment yields from Greenland glacier outlets to the ocean affect marine ecosystems by either limiting or promoting primary productivity, owing to increased turbidity and micronutrient inputs, respectively<sup>31,32</sup>. Accelerated thermal erosion of Arctic ice-rich permafrost coastlines, with coastal recession destroying hundreds of square kilometres of land per year<sup>33</sup>, is impairing infrastructure and communities<sup>34</sup>. Importantly, abrupt permafrost thaw could mobilize large amounts of organic carbon through ground collapse, landslides and erosion<sup>30</sup>, some of which will be delivered to fluvial and coastal systems and possibly increase aquatic CO<sub>2</sub> emissions and affect global carbon cycling<sup>29,35</sup>. The accelerating cryosphere degradation poses an urgent need for detailed assessments of sediment mobilization and transport processes in the world's cold regions.

In this Review, we present a global view of glacier mass loss, permafrost degradation and associated landscape changes. We detail the mechanisms of erosion and sediment transport in cryosphere-dominated regions and examine their responses to climate change and glacier–permafrost–snow melting at the basin scale. The observed changes in erosion and sediment yield in the world's cold regions are then synthesized. Finally, we conceptualize the likely future trends of sediment yields and discuss the related challenges, uncertainties and opportunities.

#### Ongoing cryosphere degradation

The cryosphere occupies approximately 30% of the Earth's land area, and melting of snow and ice dominates sediment transport in cold regions<sup>11</sup>. Since the 1950s, climate-change-driven degradation of the cryosphere (for example, glacier thinning and retreat, permafrost thaw, and snowpack reduction) has changed the magnitude and frequency of glacial floods and thermokarst dynamics, affecting sediment-transport regimes<sup>36–38</sup>. The magnitude of cryosphere change varies spatially, driven by differences in glacier and permafrost characteristics, elevation-and latitude-dependent warming rates, precipitation regime shifts, and interactions with atmospheric circulation<sup>39,40</sup>. This section describes these changes, grouped by glacial and permafrost processes.

#### Glacier mass loss and outburst floods

Although characterized by marked interannual variability and regional heterogeneity, a consistent trend of glacier recession is evident globally over the past few decades  $^{39,41,42}$  (Fig. 1). Worldwide, glacier mass has decreased at an estimated rate of  $172\pm142$  billion tonnes per year (Gt yr  $^{-1}$ ) since the  $1960s^{41}$ . Annual mass loss and recession rates have accelerated in the early twenty-first century  $^{41,42}$ , with a mean annual mass loss rate of  $267\pm16$  Gt yr  $^{-1}$  or  $0.39\pm0.12$  metres of water equivalent per year (m w.e. yr  $^{-1}$ ) over  $2000-2019^{42}$ . By the end of the twenty-first century, global glacier mass is projected to be reduced by 18-25% for the Representative Concentration Pathway (RCP) 2.6 emission scenario, with the loss of 27-33% for RCP 4.5 and 36-48% for RCP 8.5 $^{43-45}$ .

Since 2000, glacier mass loss has been greatest in Iceland, Alaska, the European Alps and the Southern Andes, at a rate of up to 0.88 m w.e. yr<sup>-1</sup>; equivalent rates in Greenland  $(0.50 \pm 0.04 \text{ m w.e. yr}^{-1})$  are close to the global average. The smallest rates of mass loss have been observed in the Russian Arctic  $(0.20-0.24 \text{ m w.e. yr}^{-1})$  and HMA  $(0.21-0.24 \text{ m w.e. yr}^{-1})^{41,42,46}$ . Locally, glacier mass gains and advancing termini have been observed in Alaska<sup>47</sup> and the Karakoram<sup>39</sup> (Fig. 1),

#### Glossary

#### Active layer

The top layer of soil or rock overlying the permafrost that experiences seasonal freeze (in winter) and thaw (in summer).

#### Basal sliding velocity

The speed of slip of a glacier over its bed, which is facilitated by lubricating meltwater and limited by frictional resistance between the glacier sole and its bed.

#### Cold regions

High-altitude and/or high-latitude low-temperature environments, where hydrogeomorphic processes are influenced by glacier, permafrost, snow, or river, lake and sea ice.

#### Cryosphere

The portion of the Earth's surface where water exists in solid form, including glaciers, ice sheets, permafrost, snowpack, and river, lake and sea ice.

#### Cryospheric basins

Basins where hydrological and geomorphic processes are influenced or even dominated by the cryosphere.

#### Glacial lake outburst floods

A flood caused by the rapid draining of an ice-marginal or moraine-dammed glacial lake, or supraglacial lake.

# Glacier equilibrium line altitudes

The elevation on a glacier where the accumulation of snow is balanced by ablation over a 1-year period.

#### Ice-free erodible landscapes

Landscapes that are not covered by glaciers and contain no ground ice, where erosion is controlled neither by glacial processes nor by other ice processes and is characterized as pluvial and fluvial processes.

#### Paraglacial erosion

Erosional processes directly conditioned by (de)glaciation, characterized by fluvial erosion and mass movements, including landslides, debris flows and avalanches.

#### Peak meltwater

The maximum of the meltwater in flux from the glacierized drainage basin; the meltwater flux initially increases with atmospheric warming and glacier melting, and then peaks, followed by a decline as glaciers shrink below a critical size.

#### Periglacial

Refers to cold and non-glacial landforms on the margin of past glaciers or geomorphic processes occurring in cold environments.

#### Permafrost

Ground, consisting of ground ice, frozen sediments, biomass and decomposed biomass, that remains at or below 0°C for at least two consecutive years.

#### Talik

A layer of soil or sediment in permafrost that remains unfrozen year-round, usually formed beneath surface water bodies.

# Thermally controlled erodible landscapes

Landscapes covered by glaciers and/or containing ground ice where erosion is dominated by glacial erosion and/or thermokarst erosion.

#### Thermokarst landscapes

Landscapes with a variety of topographic depressions or collapses of unstable ground surface arising from ground-ice thawing, including active-layer detachment, thermal erosion gullies, retrogressive thaw slumps and ice-rich riverbank collapse.

#### Yedoma permafrost

A type of Pleistocene-age permafrost that contains a substantial amount of organic material (2% carbon by mass) and ground ice (ice content of 50-90% by volume).

probably attributable to cooler summers, increased snowfall and the protection afforded by thick debris cover.

Rapid glacier retreat has increased the number and extent of supraglacial lakes and proglacial lakes, either ice-marginal or moraine-dammed<sup>48</sup> (Fig. 1). The expanding glacial lakes will increase the risk of glacial lake outburst floods (GLOFs), which can cause sudden hydrogeomorphic changes and have disastrous downstream consequences<sup>49,50</sup> (Fig. 1). From 1990 to 2018, globally the number of glacial lakes increased from 9,410 to 14,300, with their areal extent increasing from  $5.93 \times 10^3$  km<sup>2</sup> to  $8.95 \times 10^3$  km<sup>2</sup> (ref. 48). Larger glacial lakes are mainly located at mid-to-high latitudes, including northwestern North America, Greenland, Iceland, Scandinavia and the Southern Andes<sup>48</sup>. Proglacial lakes in HMA are relatively small and clustered in northern Tien Shan and the central-to-eastern Himalaya, owing to regionally faster glacier retreat there 48,51. GLOFs occur more frequently in regions with a higher density of glacial lakes and rapid glacier recession: northwestern North America, the European Alps, the Himalaya and the Southern Andes 49,50.

#### Permafrost thaw and thermokarst

Atmospheric warming and earlier seasonal snowmelt thaw the permafrost and increase active-layer thickness (ALT)  $^{52-54}$  (Fig. 2). Globally, permafrost temperatures from borehole records have warmed by  $0.29\pm0.12\,^{\circ}\text{C}$  between 2007 and 2016  $^{52}$ , accompanied by increasing ALT and decreasing permafrost extent. By the end of this century, even if

global temperature warming were limited to 1.5 °C above preindustrial levels,  $4.8 \pm 2.2$  million square kilometres of permafrost (-30% of the total) would be likely to disappear<sup>55</sup>. Over half of the existing permafrost would be degraded and the active-layer volume would expand by 4,910 km³ by 2100 under the RCP 8.5<sup>56</sup>. Large areas of near-surface permafrost would remain only in high-latitude North America and the Russian Arctic<sup>55,56</sup>.

Thawing of ice-rich permafrost has increased the extent of thermokarst landscapes and hillslope mass wasting 57-60, posing risks to nearby infrastructure and communities<sup>61</sup>. From the 1990s, 20% of the circumpolar permafrost area has been disturbed by thermokarst landscapes<sup>62</sup> in response to the amplified regional permafrost warming rate (0.39 ± 0.15 °C per decade)<sup>52</sup>. Increased incidence of thermokarst lakes, thermal erosion gullies and retrogressive thaw slumps (RTSs) have been observed in Alaska and Siberia, where yedoma permafrost is widespread<sup>58,63,64</sup>. In the Canadian Arctic, RTSs now represent the dominant geomorphic change occurring over 10% of the area of northwestern Canada<sup>65</sup>, and slump-impacted area increased fourfold around the western Canadian coasts between the 1960s and the 2000s<sup>59</sup>. Despite relatively slow permafrost warming (~0.2 °C per decade)<sup>52,66</sup>, a notable expansion of slump-impacted areas has been observed in the Beiluhe region and the Qilian Mountains on the Tibetan Plateau over the past few decades<sup>60,67</sup>.

Beyond atmospheric warming, coastal permafrost is also highly susceptible to changes in ocean temperatures and sea-ice extents<sup>68</sup>.

Along with pronounced warming of Arctic summer sea surface temperatures (-0.5 °C per decade) since the 1970s<sup>69</sup>, the sea-ice extent has declined by roughly 13% per decade<sup>69</sup> and the duration of the open-water period has extended by 1.5–2 times<sup>70</sup>. Decline in sea-ice extent is projected to continue through to the end of this century, with the annual ice-free period extending to 8 months under RCP 8.5<sup>69</sup>. The coasts of the warming Arctic Ocean are being destroyed as warmer seawater thaws coastal ground-ice bluffs<sup>71,72</sup>.

#### Changing dynamics of sediment transport

Cryosphere degradation influences sediment mobilization, transport, deposition and delivery by modifying the magnitude and timing of hydrological and geomorphic processes, changing the nature and distribution of sediment sources and sinks, and reshaping connectivity within and between hillslopes and fluvial systems. This section discusses the response of erosion processes, sediment sources and sinks, and basin-scale sediment delivery to climate change in glacierized and permafrost regions.

#### Glacierized basins

As powerful erosive agents, glaciers mobilize and transport large amounts of sediment, especially in temperate mountain regions, by glacier movement, sub- and supraglacial and ice-marginal drainage systems, and proglacial streams<sup>73-75</sup> (Fig. 3). In partially glacierized basins, erosion and sediment transport are influenced by ice dynamics and by the thermal status of the glacier, subglacial topography, bedrock lithology, glaciohydrology, and access to stored sub- and proglacial sediment<sup>9,31,76</sup>.

Glacial and paraglacial erosion. Quarrying and abrasion are the primary processes associated with glacial erosion, and both are sensitive to temperature, glacier mass balance and subglacial hydrology<sup>15,77,78</sup>. During quarrying (number 1 on Fig. 3), blocks of rock of varying sizes are plucked from the rock outcrops at the base of a glacier, forming chatter marks. If they become incorporated into the ice, they are transported down gradient by glacier sliding<sup>79,80</sup>, creating an angular blocky coarse sediment<sup>79</sup>. If not transported, eroded material will accumulate on the glacier bed, forming subglacial till. Quarrying rates scale with the number of pre-existing bedrock cracks, the crack growth rate, water pressure at the glacier-bedrock interface, bedrock strength and heterogeneity, and the basal sliding velocity<sup>78-81</sup>. With abrasion (number 2 on Fig. 3), plucked debris embedded in the glacier sole or side erodes the underlying or adjacent bedrock as the glacier moves<sup>82</sup>, forming striations on bedrock surfaces and producing fine-grained abraded sediment<sup>82</sup>. Abrasion rate is proportional to the basal sliding velocity of the glacier, the amount of basal debris, the debris-bed contact force and the bedrock's resistance to erosion<sup>82,83</sup>. Abrasion and quarrying can amplify each other: abrasion is enhanced by debris generated from quarrying, and quarrying is enhanced by the abrasion-induced increase of differential stresses74.

The overall bedrock erosion rate scales empirically with the glacier sliding velocity via a linear or power-law relationship, known as the glacial erosion law <sup>9,31,84</sup>, although there is debate as to how nonlinear this process is <sup>77</sup>. Glacier sliding velocity is regulated by glacier thermal regime (as a function of ice temperature and pressure), the subglacial hydrology and glacier mass balance <sup>74,85,86</sup>, and displays latitudinal variations <sup>15</sup>. Compared with cold-based polar glaciers, warm-based (also referred to as wet-based) temperate glaciers have lower ice viscosity and higher basal sliding velocities <sup>15,87</sup>. Glacial erosion rates range

from 0.001 mm yr $^{-1}$  for cold-based glaciers to over 100 mm yr $^{-1}$  for fast-moving temperate glaciers $^{15,74,76,88}$ . Long-term glacier mass loss can reduce the gravitational driving force and decelerate sliding $^{86}$ . However, the warming-driven increased glacier meltwater can reach the ice–bedrock interface where it can temporarily increase subglacial water pressure and lubricate the glacier base, aiding basal sliding and subglacial erosion $^{78,89}$ . Although these mechanisms have been well studied $^{90}$ , substantial uncertainties remain regarding controls on the processes and rates of glacial erosion $^{74}$ , particularly in the capacity of temperate glaciers to evacuate eroded sediment.

In a warming atmosphere, retreating glacial snouts and ice-surface lowering can expose ice-marginal bedrock, till and morainal debris to subaerial conditions. Adjacent debuttressed slopes can amplify paraglacial erosion by triggering landslides and rockfalls (number 3 on Fig. 3). In response to deglaciation, the magnitude and frequency of rockfalls have increased in North America, New Zealand, Norway and the European Alps<sup>40,91-95</sup>. Rockfalls from exposed oversteepened slopes or lateral moraines can be triggered by active freeze—thaw weathering<sup>96</sup>, ice segregation<sup>97,98</sup>, alpine permafrost thaw and intense rainfall<sup>91,94</sup>, resulting in increases of debris and sediment accumulation on the glacier surface (number 4 on Fig. 3) and at the glacier margins<sup>99,100</sup>.

**Subglacial sediment transport.** The importance of subglacial drainage systems in glacier basal sliding, subglacial erosion and sediment transport has been increasingly emphasized<sup>74,75,101</sup>. Subglacial channelized drainage systems are effective in evacuating subglacially eroded sediment, especially coarse sediment<sup>101–103</sup>, although they are spatially limited and will shrink as glaciers thin.

With increased melting, newly generated and expanded crevasses and moulins (numbers 5 and 6 on Fig. 3) on the surface of glaciers and ice sheets can boost surface-to-bed water transfer by forming nearvertical conduits connected to distributed englacial water routing networks<sup>104–106</sup>. The drainage from supraglacial lakes and streams (number 7 on Fig. 3) through pre-existing englacial fractures opens new vertical hydro-connections, possibly causing transient ice-bed separation, ice uplift and water pulses, and carving new bedrock channels 107,108. Subglacial drainage systems promoted by surface-to-bed water transfer can increase subglacial abrasion by sediment-bearing flows and effectively remove protective sediment from bedrock surfaces, although erosion rates associated with subglacial meltwater can be up to two orders of magnitude lower than those for glacial erosion  $^{75,101}\!.$  Furthermore, subglacial lake outbursts can surcharge subglacial drainage systems, flush out subglacial sediments, and affect proglacial hydrogeomorphic environments, forming outwash fans at glacier margins and aggrading existing proglacial channels 109,110.

Access to stored amounts of sediment and till is also important in subglacial sediment evacuation <sup>12</sup>. Glacier equilibrium line altitudes can progressively retreat upslope during deglaciation, and the accessibility of subglacially stored sediment increases by exposing large amounts of previously buried sediment (glacial tills, number 9 on Fig. 3) to the upward extended subglacial drainage networks <sup>12</sup>. As the glacier equilibrium line moves upward, increased meltwater can access subglacial tills at higher elevations and remove stored sediment, promoting glacial bedrock erosion until the glacier is smaller than a critical size <sup>12</sup>.

**Sediment delivery in response to deglaciation.** As glaciers retreat, they commonly leave behind abundant readily transportable sediment for a transient period (for example, decades or centuries), and then these deposits are progressively mined, leaving a supply-limited

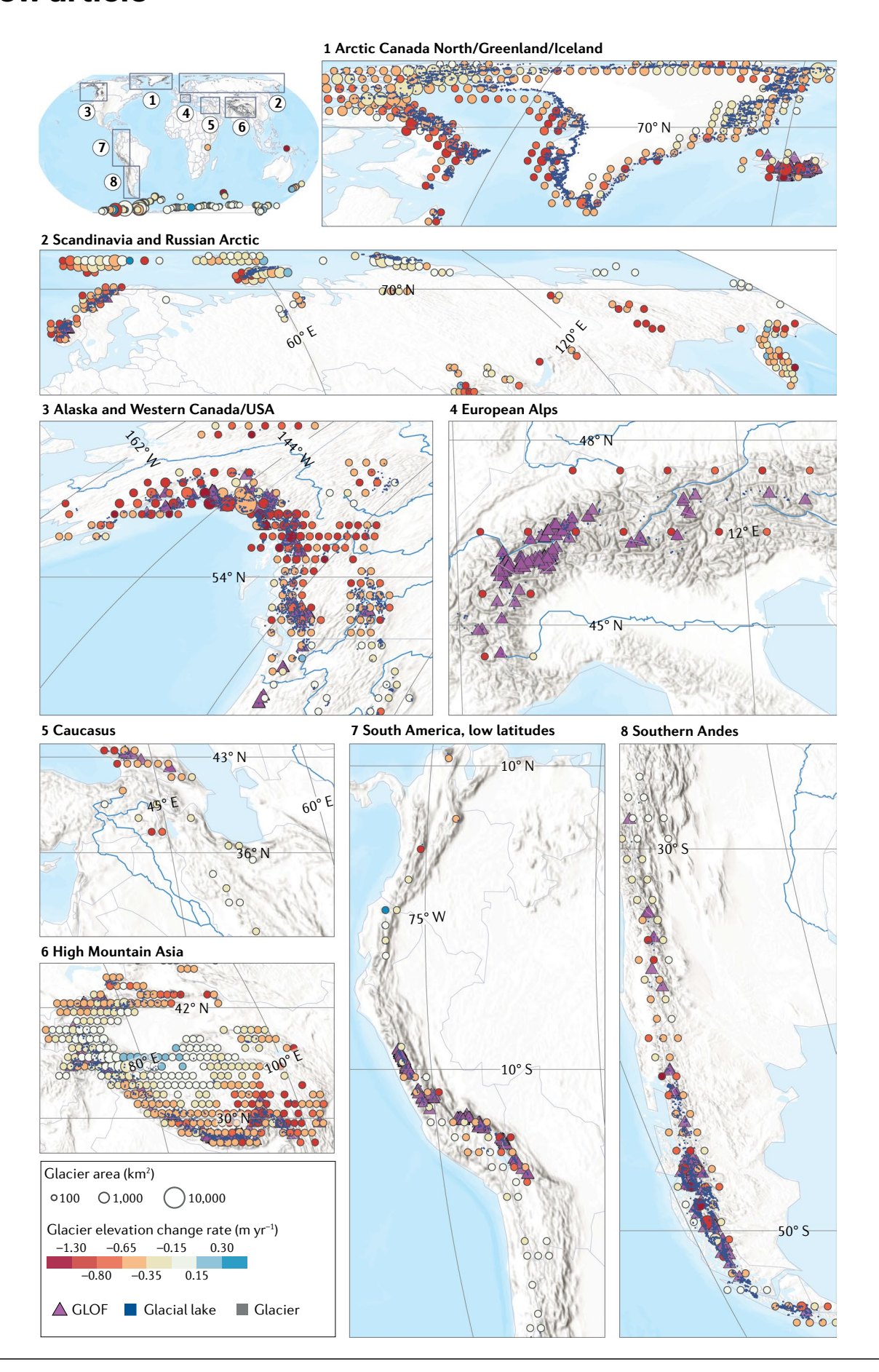


**Fig. 1**| **Glacier melt.** Most cold regions have experienced rapid glacier mass loss over the past two decades, accompanied by glacial lake expansion and glacial lake outburst floods (GLOFs). Glacier coverage is based on the Randolph Glacier Inventory (RGI) 6.0 dataset<sup>238</sup>. Circle colour represents glacier elevation change rate (m yr<sup>-1</sup>) between 2000 and 2019 aggregated for 1° × 1° grids within a 90%

confidence interval, and circle sizes represent the glacier area<sup>42</sup>. Violet triangles mark locations of recorded GLOFs, with 2,560 GLOF events identified from more than 340 glacial lakes since the 1500s and 1,977 GLOFs occurring after the 1900s<sup>50</sup>. GLOF events triggered by earthquake and geothermal activity have been excluded. Glacial lakes mapped from 2015 to 2018<sup>48</sup> are shown as blue dots.

environment<sup>111</sup>. Most of this sediment is not rapidly transferred downstream but remains as moraines, debris cones and alluvial fans in the proglacial zone<sup>14</sup>. During intense melting or extreme rainstorms, this sediment deposited near the glacier terminus may be remobilized and delivered downstream<sup>111-113</sup>.

The transport efficacy and storage of sediment mobilized by glacier erosion are largely influenced by glacier melt volume<sup>114</sup> and glacier-channel connectivity<sup>7,36</sup>. As glaciers recede, gullies extend upslope and enhance sediment connectivity and delivery by reducing dependence on supra/subglacial transport and expanding the contributing area<sup>7,14,115</sup>. However, export of glacial sediment downstream is modulated by sediment sinks (notably, proglacial lakes, number 8 on Fig. 3)<sup>116,117</sup> and disconnections (for example, moraines or alluvial fans)<sup>14</sup>, creating transient disconnectivity<sup>7,36</sup>. Proglacial lakes have been increasing worldwide<sup>48</sup> and can trap large proportions of the sediment mobilized by glaciers (40–80%) and act as first-order sediment sinks<sup>116</sup>.

Whereas proglacial lakes generally trap sediment, GLOFs are distinctive agents of sediment delivery far outpacing other erosion processes, owing to the high stream power. GLOFs enhance channel erosion by mobilizing channel-defining coarse sediment and deliver large amounts of sediment downstream 118-120. Sudden drainage of glacial lakes is often associated with order-of-magnitude increases in discharge 22,49,50. Powerful streamflow pulses in a GLOF water bore mobilize and transport channel-defining boulders that are rarely affected by more conventional floods<sup>118,119</sup>. Once armouring boulders are removed, large amounts of unconsolidated sediment can be mobilized from the underlying river channels, accompanied by bedrock erosion and lateral riverbank erosion<sup>121,122</sup>. A 2016 GLOF in Nepal<sup>118</sup> affected a 40-km stretch of river channel by downcutting the riverbed by 1-10 m, widening the channel by 40%, causing 26 channel-connected landslides and a 30-fold increase in sediment flux. Although the substantially increased sediment flux associated with GLOFs gradually reverts to near the original level, erosion and deposition during GLOFs and associated geomorphic adjustments can cause severe, long-lasting consequences downstream 119,123.

With ongoing deglaciation and commonly increased precipitation extremes<sup>40,124</sup>, sediment yield from glacierized basins will initially increase, driven by increased glacial erosion and sediment supply<sup>125,126</sup>, easier access to subglacial tills<sup>12</sup>, increased transport capacity and increased incidence of extreme floods. A subsequent sediment decrease reflects declining glacier mass and meltwater, decelerated glacial erosion<sup>86,117</sup>, decreased freeze–thaw weathering at lower elevations<sup>127</sup> and vegetation colonization (Fig. 3).

#### **Permafrost basins**

In response to atmospheric warming and precipitation extremes <sup>3,65</sup>, permafrost thaw and the intensity of thermokarst erosion have intensified in many permafrost regions. The associated release and mobilization of stored sediment increase fluvial sediment loads <sup>37,128</sup>. Permafrost degradation affects fluvial sediment fluxes by expanding the extent of erodible thermokarst landscapes, and by changing the density and spatial distribution of flow paths and therefore sediment connectivity <sup>1,57,65,129</sup> (Fig. 4). The impact of permafrost on hydrogeomorphic processes can be subdivided into physical disturbance (numbers 1–7 on Fig. 4, showing visible landscape changes) and thermal disturbance (number 8 on Fig. 4, showing no visible geomorphic changes) <sup>20,37,130</sup>. Among the

processes involved, active-layer detachment, thermal erosion gullies, retrogressive thaw slumps and fluvio-thermal erosion (FTE) are the primary sediment sources  $^{13,131-133}$ .

Permafrost erosion. Active-layer detachment (ALD) represents the occurrence of landslides on low-angled permafrost slopes with the thawed active layer sliding downslope (number 1 on Fig. 4)<sup>134</sup>. ALD can be initiated by deep active-layer thaw during warm summers or excessive porewater pressure caused by heavy rainfall or snowmelt<sup>17,134,135</sup>. Once initiated, ALDs can continue downslope for hundreds of metres, with a long-distance impact on sediment mobilization and transport<sup>136</sup>. Expanded scar zones with ALDs extending downslope expose the underlying permafrost and accelerate thawing<sup>17</sup>. The exposed ground ice can trigger thaw slumps, amplifying disturbances<sup>137</sup>, or cause land subsidence, trapping sediment in the scar zone<sup>136</sup>. Newly available sediment can cause long-lasting increases in downstream sediment fluxes when transported by rainfall runoff or meltwater and sustained by hydrogeomorphic connectivity<sup>131</sup>.

Thermal erosion gullies (TEGs) initiate by surface heat melt of ground ice and by surface flow incising into high-ice-content permafrost. TEGs commonly occur on permafrost slopes (number 2 on Fig. 4) or within eroded ice-wedge polygons (number 6 on Fig. 4)<sup>132,138</sup>. Once initiated, TEGs can lengthen by hundreds of metres and widen substantially through lateral erosion and headward erosion <sup>138</sup>, because of ground-ice melting<sup>63,132,138</sup>. Lateral and headward erosion of TEGs can trigger channel-connected permafrost collapses and slumps<sup>137</sup> and link upslope sediment sources with downstream river channels<sup>138</sup>, notably increasing slope channelization and sediment supply. The shortened flow path by TEGs accelerates the response of sediment fluxes to hydrological changes and permafrost disturbance<sup>132,135</sup>. Additionally, vegetation and wetlands can degrade by TEG development, which can further increase erosion rates along TEGs through positive feedback<sup>139</sup>.

Retrogressive thaw slumps (number 3 on Fig. 4) are important sediment sources in ice-rich permafrost and are sensitive to climate change<sup>59,129</sup>. Increasing incidence of RTSs has been reported in permafrost environments worldwide, including the  $\operatorname{Arctic}$  and the Tibetan Plateau, driven by atmospheric warming and increased summer rainfall<sup>3,59,67</sup>. RTSs show seasonal cycles and initiate in summer by melting of exposed ground ice in a headwall<sup>3</sup>. The meltwater then mobilizes debris and soil from the headwall 128,129. RTSs stabilize in autumn, owing to lower temperatures ceasing ice melting and accumulated sediment covering the ice<sup>3</sup>. They can remain active and expand for years to decades, if the mobilized material continues to be transported downslope and exposed headwalls are still ice-rich<sup>3,140</sup>. Channel-connected RTSs have been found to increase downstream sediment loads by orders of magnitude<sup>128,129</sup>. Development of RTSs is intensified by extreme rainstorms<sup>3</sup>, lateral heat exchange along riverbanks or lakeshores<sup>141</sup>, other landscape disturbances<sup>137</sup> and permafrost shoreline retreat<sup>142</sup>.

Fluvio-thermal erosion (number 4 on Fig. 4), or thermal bank erosion, is erosion by moving water that thaws frozen substrate and melts ground ice along a riverbank<sup>143</sup>. With earlier ice breakup, warming river water temperatures and increasing water discharge, FTE has been increasingly observed in Alaska, Arctic Canada, and Siberia<sup>63,144–146</sup>. Riverbank permafrost thawing is dominated by conductive heat

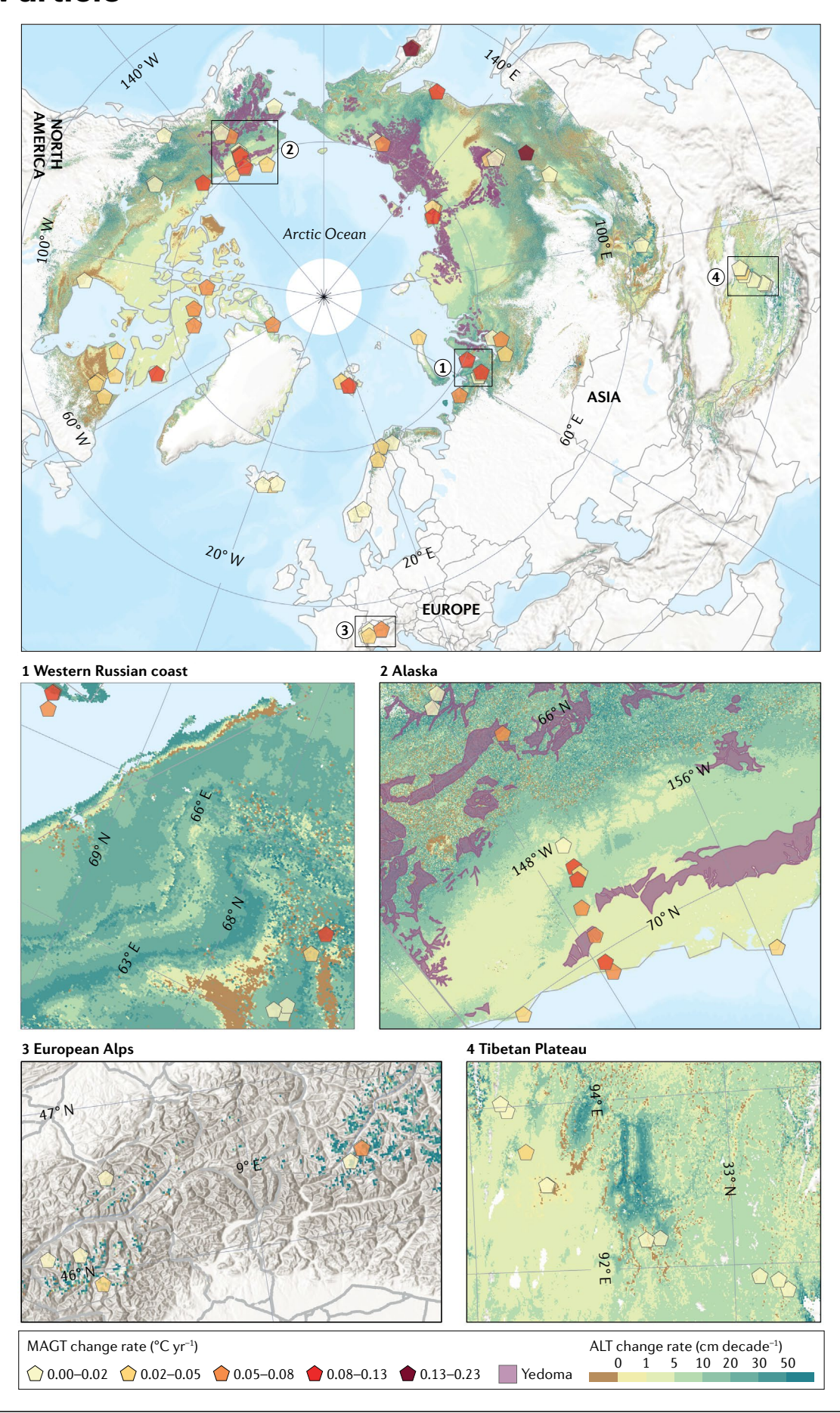


**Fig. 2**| **Permafrost thaw in the Northern Hemisphere.** Permafrost has been warming and the active layer has been thickening over the past two decades. Warming trends in mean annual ground temperature (MAGT) near the depth of zero annual amplitude from 2007 to 2016 illustrated by 104 boreholes, drilled to depths of 5–30 m (ref. <sup>52</sup>). Deepening of active-layer thickness (ALT)

over 1997–2019 estimated from the Northern Hemisphere ALT data released by the European Space Agency's Climate Change Initiative Permafrost project<sup>239</sup>. The statistical significance (p-value) of ALT change rates is shown in Supplementary Fig. 1. Yedoma permafrost is highlighted in violet<sup>240</sup>.

exchange between warmer river water and frozen banks<sup>54,63,141</sup>. Once FTE begins, formation of thermo-erosional niches at the base of the riverbank reduces bank stability, causing collapse<sup>146-148</sup>. During high flows, this readily available sediment and abundant organic matter of the typically peaty floodplain or bar surfaces can be rapidly transported by the flowing water<sup>143</sup> and increase sediment and carbon loads substantially 144,145. The efficacy and magnitude of FTE are influenced by factors including the presence of river ice, river water temperature and discharge<sup>145,148</sup>. During the early melt season, drifting ice can remove the riverbank protective layer by abrasion, undercutting and gouging, exposing the underlying bank to fluvial entrainment<sup>149</sup>. For rivers of warm water, ice breakup pulses can cause FTE owing to substantial increases in water levels and discharges and expanded contact with the floodwater 150,151. FTE can also gradually stabilize owing to decreased ground-ice exposure caused by sediment deposition at the base of the riverbanks and on their flattened profiles 63,147.

Sediment delivery in response to thermokarst processes. Permafrost thaw expands thermokarst landscapes and creates active sediment sources 13,34,152. The efficacy of sediment mobilization and delivery downstream from the disturbed permafrost area is governed by basinscale hydrogeomorphic connectivity<sup>129,153</sup>. New gullies and expanded flow paths during intense rainfall or high meltwater increase sediment conveyance by enhancing hillslope-channel coupling, reworking previously stored sediment and linking disconnected sediment sources (for example, hillslope RTS and ALD, Fig. 4)8,129. Such increased connectivity facilitates a sediment cascade and transmits the signal of disturbance downstream<sup>8,19,140</sup>. However, the signal generated by upstream permafrost disturbance and degradation can be disconnected from downstream areas and the catchment outlet by local sediment sinks, including expanded areas of thaw subsidence <sup>136</sup> (number 7 on Fig. 4), thermokarst lakes<sup>58</sup> (number 5 on Fig. 4), and debris tongues accumulating within the disturbed area 140.

Permafrost thaw can also dampen sediment transport by altering soil permeability, surface/subsurface flow paths and hydrological connectivity<sup>130</sup>. Despite the likely increase of overall sediment-transport capacity due to extension of the melt season, more extreme rain and melting of ground ice, potential loss of peak meltwater capacity in the melt season due to enhanced water infiltration can decrease sediment-transport capacity<sup>154,155</sup>. With permafrost thaw, talik enlargement and breakthrough can increase the connection between surface water and groundwater<sup>154,156</sup>.

Permafrost disturbance is likely to increase nonlinearly in a changing climate, causing disproportionate increases in fluvial fluxes and downstream impacts<sup>3,65,140,157</sup> until thermokarst landscapes stabilize. The continued melting of ground ice should increase sediment availability through the development of more erodible and accessible thermokarst landscapes and should boost slope-channel connectivity<sup>3,157</sup> (Fig. 4). Increased precipitation intensity<sup>124</sup> could intensify permafrost erosion by triggering mass movements, remobilizing deposited sediment and further accelerating permafrost thaw via lateral heat exchange<sup>19</sup>.

**Erosion along permafrost coasts.** Sediment mobilization along permafrost coastlines is characterized by the complicated interplay of permafrost status and thermokarst development, sea-ice extent,

open-water periods, wave and storm activities, and sea level rise<sup>68,158</sup>, making it distinct from permafrost hillslope processes. Thermodenudation of the bluff top and thermo-abrasion of the bluff base represent the primary sediment mobilization processes from ice-rich permafrost coasts<sup>159</sup>. Thermo-denudation driven by intensified solar radiation and heat conduction ablates the ground ice, reduces the cohesion of ice-bonded bluff slopes and triggers coastal recession by ALDs, RTSs and ground subsidence<sup>142,160</sup>. Ice-rich bluffs can contain up to 65% ice, so most melt results in water; the remaining thawed sediment are delivered to the bluff base by meltwater and gravity<sup>159</sup>.

In contrast, thermo-abrasion includes both thermal erosion by seawater and mechanical erosion by wave action <sup>161</sup> and is pronounced in coasts with high ground-ice content experiencing decreased sea ice, higher wind-wave energy and storm surge setup <sup>162</sup>. The landward recession of bluff toes during thermo-abrasion commonly forms thermoniches and related block failures <sup>72,163</sup>, substantially increasing coastal erosion rates and introducing sediment and carbon into the offshore system <sup>72,159</sup>. Erosion along ice-rich permafrost coastlines outpaces mechanical erosion along non-permafrost coasts <sup>33,68</sup>. The mass-wasting processes initiated by thermo-abrasion tend to dominate the erosion and shape coastal morphology along high-latitude coasts in response to ocean warming <sup>72</sup>. Whereas coastal bluffs can contain peaty and organic-rich layers, inventories of bluff substrate characteristics and coastal erosion rates have shown that carbon fluxes to the ocean from coastal erosion are lower than riverine transport <sup>164</sup>.

#### Observed increases in sediment fluxes

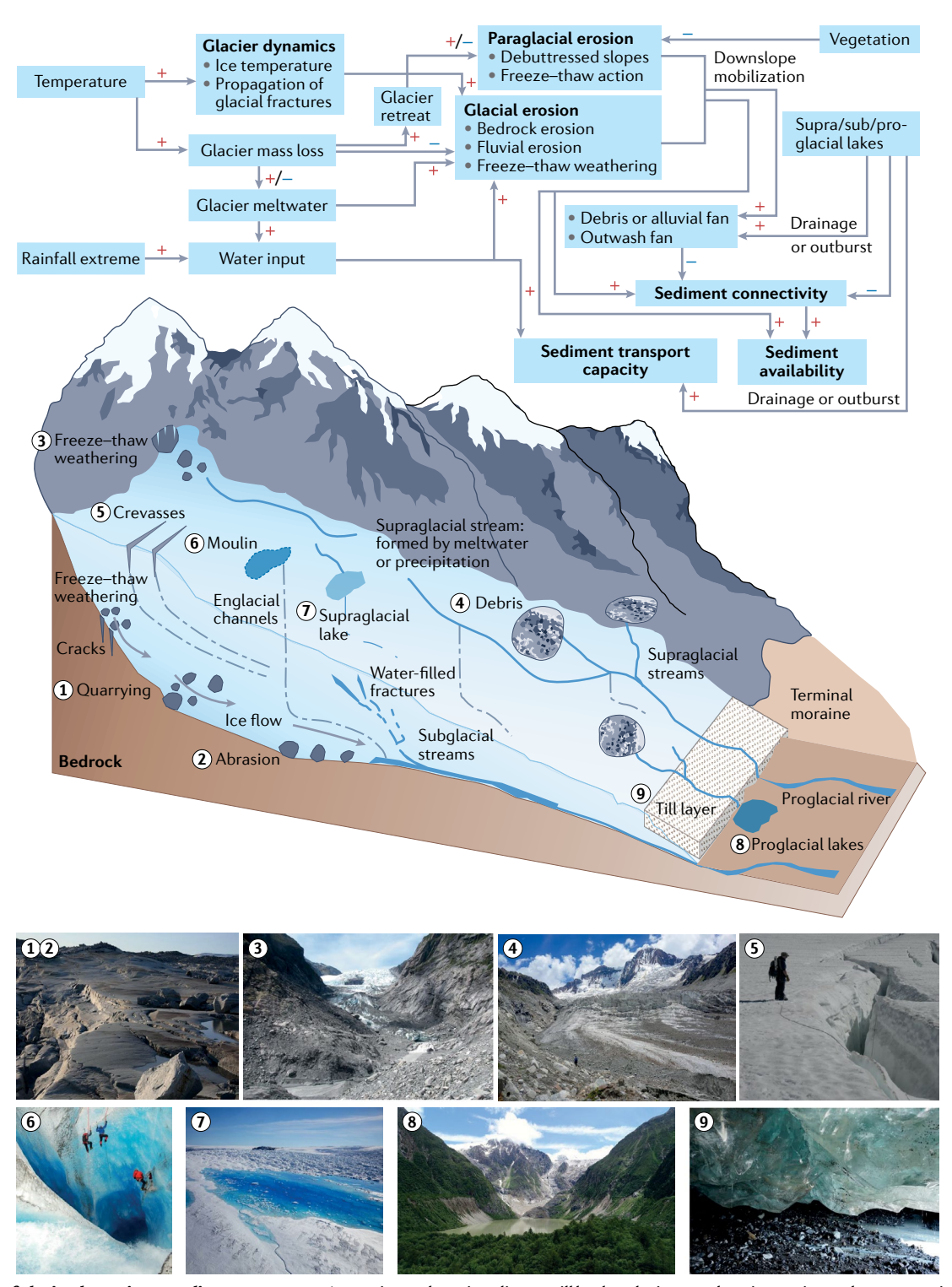
Increased erosion and basin-scale sediment yields are observed in the world's cold regions, driven by rapid cryosphere degradation<sup>1,4,140</sup>. A compilation of 76 locations shows upward trends in sediment fluxes (suspended load, bedload, particulate organic carbon and riverbank/ slope erosion) from over 50 studies (Fig. 5a and Supplementary Table 1). The global distribution of such evidence is influenced by established sediment-monitoring programmes and published data, and is biased towards suspended sediment (53 locations) with far fewer studies of bedload (15 locations) or erosion rates (8 locations; Supplementary Table 3). Observed locations do provide evidence from the high Arctic, European mountains, HMA and Andes (Fig. 5a). Few studies documented decreased sediment fluxes (for example, the Swiss Alps and northern Alaska)<sup>147,165</sup> (Supplementary Fig. 2), which could reflect field sampling bias toward regions where negative impacts of increasing sediment flux were suspected.

#### Observations from thermokarst basins

Expanding thermokarst landscapes are thought to be responsible for increased riverbank erosion and sediment yields from the Canadian and Siberian Arctic, Alaska and the Tibetan Plateau (Fig. 5a), the released organic carbon and nutrients further affecting thermokarst ecosystems  $^{30,166}$ . In the eastern Lena Delta, erosion rates along yedoma permafrost riverbanks increased three-fold between the 1960s and 2010s, and the amount of organic carbon and nitrogen released into the rivers more than doubled  $^{167}$ . Along an actively eroded bluff (150 m) of the Itkillik River in Alaska, the yedoma riverbank retreated at an accelerated rate, reaching 20 m yr  $^{-1}$  between 2007 and 2011, and annually released -70,000 t of sediment (including 880 t of organic carbon) into the river  $^{63}$ . Channel-connected thaw slumps in northern Canada have

increased sediment yields by up to three orders of magnitude compared with undisturbed basins<sup>128,129,140</sup>. Active-layer detachments reported from small watersheds in the Canadian High Arctic (Melville Island)

caused a 30-fold increase in sediment flux during an anomalously warm year, followed by multiyear recovery<sup>131</sup>. In the Tibetan Plateau, permafrost thawing and associated expansion of erodible landscapes have



 $\textbf{Fig. 3} \ | \ \textbf{Impacts of glacier dynamics on sediment transport.} \ A \ warming \ and \ wetting \ climate \ will lead to glacier \ mass loss, increasing \ meltwater, erosion \ and \ sediment \ transport initially, followed by an eventual meltwater decline \ and \ sediment \ exhaustion. Positive \ relationships \ between \ variables \ are \ noted \ by \ a+sign, \ negative \ relationships \ by \ a-sign. \ Field \ photos \ (numbered \ 1-9) \ depict \ the \ main \ glacial \ erosion \ processes \ and \ features \ in \ the \ diagram.$ 

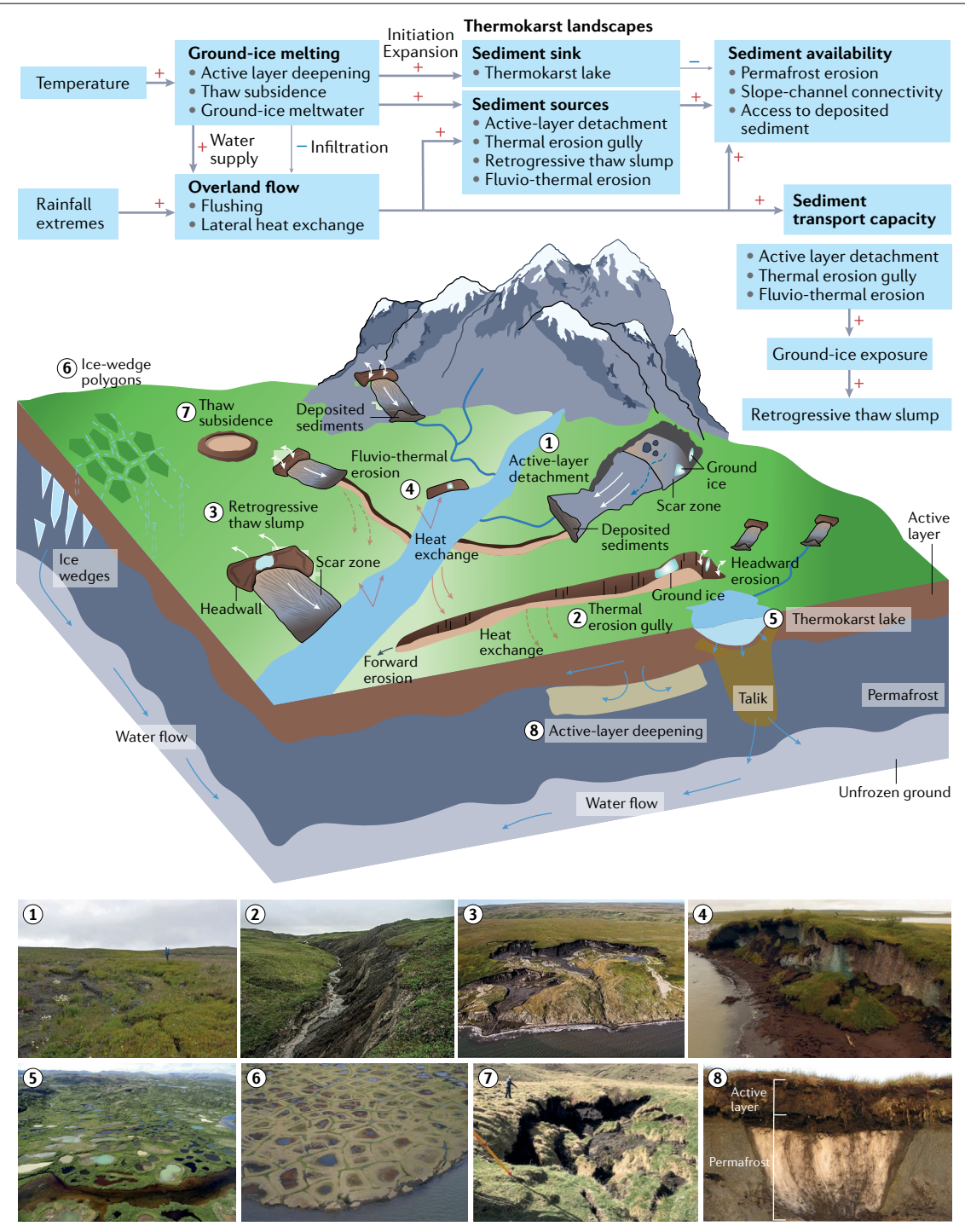
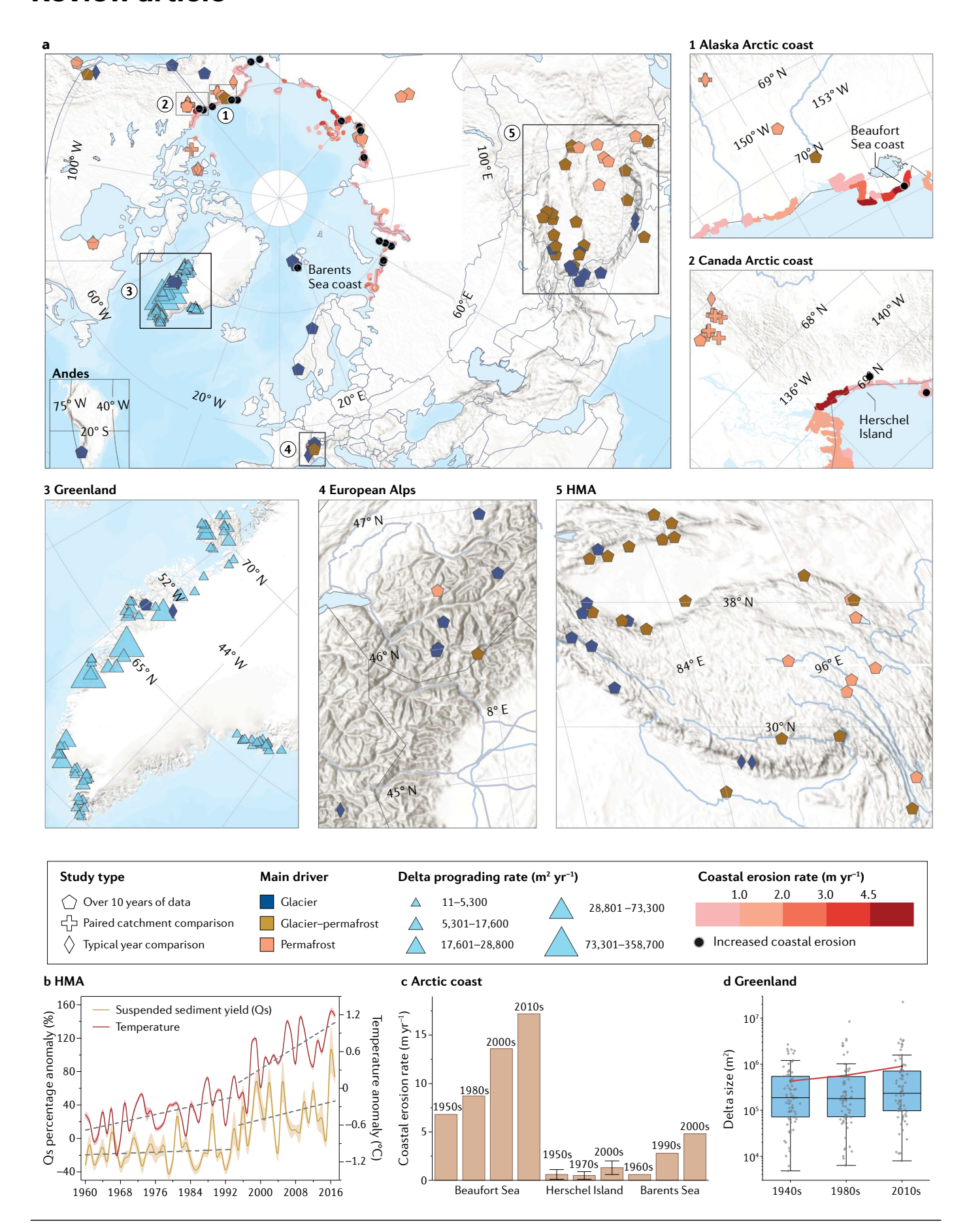


Fig. 4 | Impacts of permafrost degradation and thermokarst processes on sediment transport. Thermokarst processes related to a warming and wetting climate will increase the occurrence of mass movements until the slopes are stabilized. Positive relationships between variables are noted by a + sign, negative relationships by a – sign. Field photos (numbered 1–8) depict key features of thermokarst landscapes, and related permafrost erosion processes are depicted in the central panel. Solid blue lines represent the small channels formed by meltwater or rainfall. Dashed blue lines within ice-wedge polygons represent

eroded gullies associated with ground-ice melting. Solid brown arrows represent the lateral heat exchange along riverbanks. Dashed brown arrows represent the lateral heat exchange along gullies. Photos 1–3 reprinted with permission from ref.<sup>133</sup>; Photo 4 courtesy of M. Roger/Natural Resources Canada; Photo 5 courtesy of Jérôme Comte, Institut national de la recherche scientifique and Centre for northern studies; Photo 6 courtesy of B. Richmond/A. Gibbs, US Geological Survey; Photo 7 courtesy of L. Huang; Photo 8 courtesy of Benjamin Jones.



**Fig. 5** | **Increased sediment fluxes due to modern climate change and cryosphere degradation. a**, Seventy-six locations show increased sediment fluxes due to enhanced glacier melting, permafrost disturbance and combined glacier–permafrost impact. Among these, increased sediment fluxes at 57 locations (75%) are determined from decadal observations; increases at 10 locations from paired catchment comparisons (comparison of sediment fluxes from areas disturbed by glacier/permafrost-related processes with an undisturbed region); and 9 locations from typical year comparisons (sediment fluxes in a normal year versus sediment fluxes in a disturbed year). Erosion rates along Arctic permafrost coasts are sourced from ref. <sup>33</sup>, with accelerated coastal erosion rates observed in 18 locations (details in Supplementary Tables 1 and 2). Magnitudes of Greenland delta progradation from the 1940s to 2010s are

sourced from ref.<sup>4</sup>. Subpanels for region 5 and the Andes have been reprojected to the Equal Earth map projection to provide more intuitive visualization. HMA, High Mountain Asia. **b**, Accelerated increases in annual suspended-sediment yield (Qs, as percentage) and temperature anomalies in HMA over 1960–2017<sup>1</sup>. Shaded areas denote standard errors. Trends of Qs and temperature anomalies are fitted separately for 1960–1995 and 1995–2017 (grey dashed lines). **c**, Intensified erosion rates along Arctic permafrost coasts: Beaufort Sea coast, Alaska<sup>72,183</sup>; Herschel Island coast, northern Canada<sup>163</sup>; and Barents Sea coast, northeastern Russia<sup>182</sup>. **d**, Expanded Greenland delta area from the 1940s to 2010s<sup>4</sup>. Grey dots represent individual deltas; central horizontal black lines represent median values. The change in mean delta size of each period is shown as the red line.

doubled the sediment yield in a headwater of the Yangtze between 1985 and  $2016^{168}$ ; and led to an eightfold increase in sediment yield around Qinghai Lake between the 1990s and  $2010s^{169}$ .

#### Observations from glacierized basins

Increased erosion and sediment yields from European mountains, the Himalaya and the Andes are mainly induced by increased subglacial sediment evacuation and unstable hillslopes (Fig. 5a), threatening downstream infrastructure and communities 23,170,171. In the Italian Alps, warming temperatures have been locally linked to an order-ofmagnitude increase in erosion from high periglacial terrain<sup>172</sup>. A near doubling of coarse sediment yield has been observed in two partially glacierized basins in the western Swiss Alps in response to glacier recession<sup>7,36</sup>. In Norway, the sedimentation rate of a proglacial lake has accelerated since the 1970s in response to accelerating glacier retreat <sup>173</sup>. In European mountains, increased reservoir sedimentation has reduced the lifetime of hydropower infrastructure, and more frequent sediment flushing of hydropower installations has demonstrated negative impacts on instream ecosystems<sup>171</sup>. In the Chandra River, western Himalaya, the sediment yield doubled between the 1980s and 2010s, associated with a 65% reduction in low-elevation glacier volumes<sup>174</sup>. The increased channel and floodplain deposition in less-steep areas downstream can elevate the riverbed and potentially trigger river avulsions and flooding<sup>170,175</sup>. Rapid glacier recession in the Southern Andes has caused a sixfold increase in frequency of extreme turbidity events. affecting water quality in the nearby megacity of Santiago<sup>23</sup>. Although sediment yields in response to longer-term deglaciation since the Last Glacial Maximum have rarely been observed globally, state-of-theart conceptual models<sup>75,176,177</sup> and sediment-core analysis<sup>178,179</sup> show nonlinear increases in erosion and sediment-related yield in the early phase of deglaciation, followed by rapid decline late in deglaciation as landscapes stabilize.

#### Observations from polar basins

Extensive erosion has occurred along Arctic coastlines due to rapid thawing of ice-rich permafrost \$^{3,68,158,161}\$, with sediment-associated nutrient inputs sustaining 20% of the net primary production of the Arctic Ocean \$^{180}\$. Since the early twenty-first century, amplified atmospheric warming has accelerated erosion rates in 18 out of 20 coastal permafrost locations in Alaska, northwestern Canada and the East Siberian Arctic (Fig. 5a,c and Supplementary Table 2), enhancing land—ocean biogeochemical fluxes \$^{180}\$ but threatening coastal infrastructure \$^{158,161,181}\$. Specifically, a sevenfold increase in coastal erosion rate has been observed along the Barents Sea coast (Western Russian Arctic) between the 1960s and 2000s \$^{182}\$. Erosion rates along the Beaufort Sea coast (Alaskan Arctic) and Herschel Island (Canadian Arctic) have doubled since the 1950s  $^{163,183}$  and accelerated erosion is amplified by the increased incidence of coast-connected thermokarst landslides ( $^{-140}$ %)  $^{142}$ .

Erosion and irreversible land loss cost billions of dollars for relocating or protecting infrastructure  $^{34,161}$ , and conflict with future anticipated economic development of the Arctic coastline, including the expansion of ports and shipping, and oil and gas exploitation.

Mass loss from the Greenland Ice Sheet since the 1960s has caused a 56% increase in suspended-sediment delivery to adjacent proglacial rivers and coastal zones  $^{31,184}$ . The increased sediment flux outpaces delta erosion and stagnation due to sea level rise  $^{4,185,186}$ , thus prograding the deltas of southern Greenland by 110% between the 1940s and 2010s  $^{4}$  (Fig. 5d). The progradation of Greenland's deltas emphasizes the role of land–ocean sediment flux in sustaining deltas and what could be seen as a longer-term benefit of terrestrial cryosphere degradation  $^{4,187}$ .

#### **Projections and peak sediment**

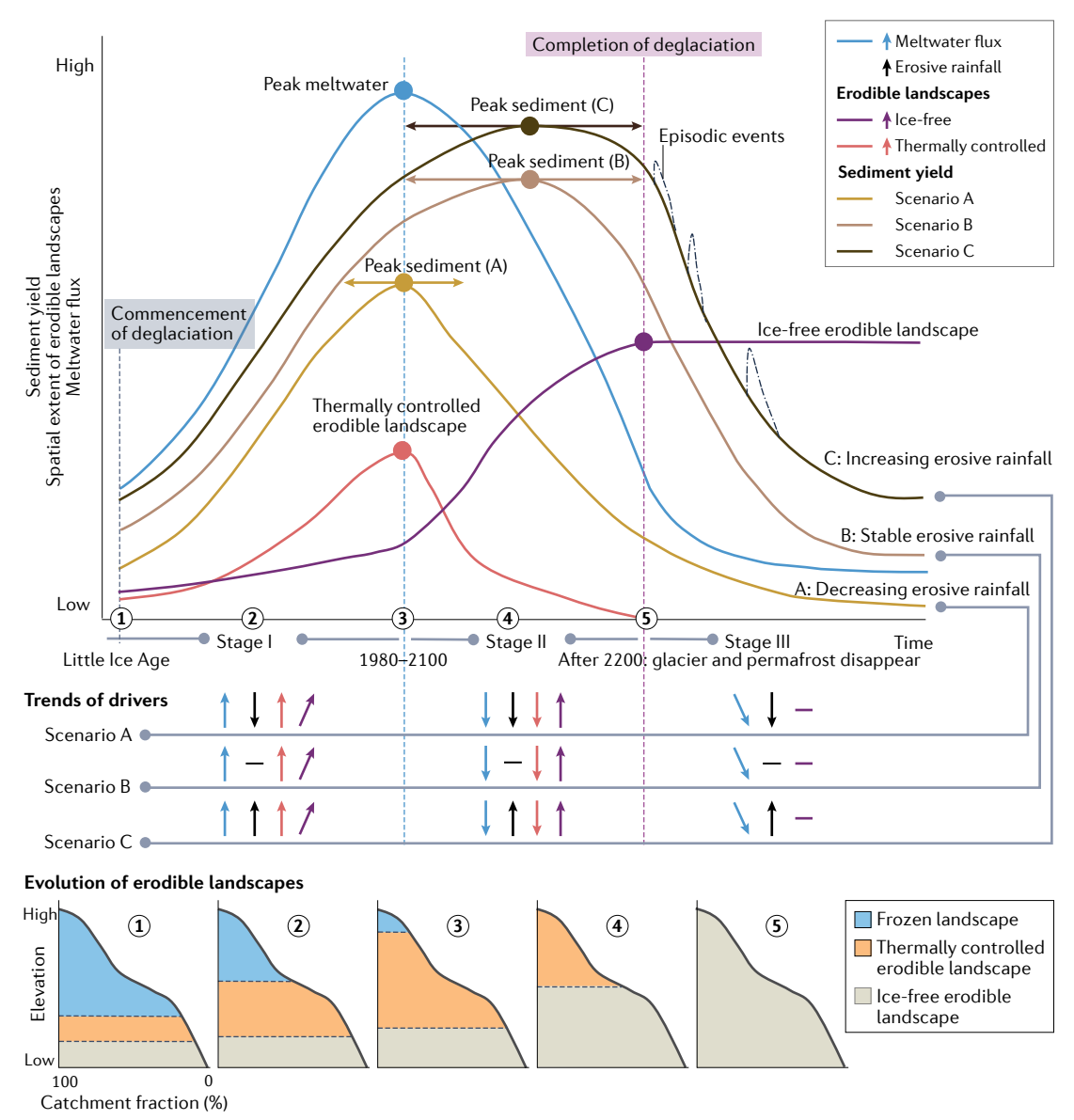
Ongoing climate change is likely to initially increase sediment yields in pristine cold environments, in response to glacier melting and permafrost thaw. Sediment yield will eventually reach a maximum 75,176, herein referred to as 'peak sediment', followed by declining sediment yields as the areas contributing sediment shrink. Ongoing cryosphere degradation will also cause a shift in the sediment-transport regime and seasonal pattern 37,188. The timing of the sediment regime shift and the tipping point of sediment yield will be jointly regulated by trends in meltwater runoff, erosive rainfall and the extent of thermally controlled erodible landscapes and ice-free erodible landscapes 13,75,88 (Fig. 6). This section qualitatively speculates on the likely evolution of future sediment yield in response to global warming in large cryospheric basins.

Globally, nearly half of the large-scale glacierized basins have already passed peak meltwater and entered the declining meltwater phase; the tipping points in most remaining basins are projected to be reached before 2100<sup>11</sup>. The completion of deglaciation could occur after the year 2200, with Arctic and Antarctic ice sheets and Arctic permafrost existing beyond 2200<sup>189–191</sup>. Compared with the hydrological impacts of deglaciation, landscape changes are understudied and more complex to project<sup>88</sup>. Theoretically, active thermally controlled erodible landscapes, as a function of temperature and ice content (glacier or ground ice)<sup>13</sup>, will peak at the time of peak meltwater and then decline to zero at the completion of deglaciation, concurrently with ice-free erodible landscapes expanding. Once a zone becomes ice-free, landscapes stabilize at differing rates depending on the deglaciated landforms, geomorphic feedbacks and landcover changes<sup>177,192</sup>.

By reflecting changes in meltwater and erodible landscapes, sediment-transport regimes could shift through three temporal stages separated by the timing of peak meltwater and completion of deglaciation (Fig. 6), regardless of glacier re-advance, (dis)connectivity changes, scale and/or threshold effects in sediment transport, the stabilization rate of deglaciated landscapes, and human interference. In stage I, the sediment regime is dominated by thermal processes,

including thermally activated glacier/permafrosterosion and meltwater-driven sediment transport<sup>13,18,193</sup>. Readily erodible sediment from freshly deglaciated regions and thermokarst hillslopes, combined with enhanced transport capacity by meltwater, will probably increase sediment yield in the early stage of deglaciation<sup>75,88</sup>. In stage II, reduced meltwater would render rainfall runoff increasingly important in

sediment mobilization and transport, and the sediment regime would be controlled by coupled thermal and pluvial processes<sup>19</sup>. The trend of changes in sediment yield would reflect the interplay of reduced meltwater, continuously exposed proglacial and/or periglacial sediment sources, and changes in erosive rainfall<sup>11,177</sup>. In stage III, fully exposed erodible ice-free landscapes and depleted meltwater after the



 $\label{eq:Fig.6} \textbf{Peak sediment and transport regime changes.} Sediment-transport regimes shift under a warming climate, in three stages: stage I, thermally controlled; stage II, thermally and precipitation-controlled; and stage III, precipitation-controlled, where pluvial processes, such as extreme rainfall and flooding, dominate. The timing of peak meltwater is inferred from a global-scale assessment of glacierized basins $^{11}$, wherein the timing of completion of deglaciation is inferred from regional projections of cryosphere degradation $^{189-191}$. The concept of peak sediment refers to refs. $^{75,176}$ and further incorporates the constraints of thermally controlled and ice-free erodible landscapes, meltwater flux and various rainfall scenarios in the upper panel. The three brown curves represent sediment fluxes and the timing of peak sediment under different$ 

erosive rainfall scenarios: A (decreasing), B (stable) and C (increasing). The timing and potential time range of the peak sediment flux are marked by the solid circle and arrows, respectively. The basin hypsometry shown in the bottom panel represents the evolution of erodible landscapes during deglaciation, with the ice-free area in brown, the area with active thermally controlled erosion in orange, and the frozen area with less effective erosion in blue. This projection of future sediment yield ignores glacier re-advance during cooling periods, (dis)connectivity changes, scale and threshold effects in sediment transport, the stabilization rate of deglaciated landscapes, and human interference; and refers to relatively large mountainous cryospheric basins (larger than  $1,000 \, \mathrm{km}^2$ ).

completion of deglaciation would shift the sediment-transport regime towards a precipitation-dependent regime with pluvially controlled sediment mobilization, followed by an eventual decline in sediment yield due to sediment supply exhaustion 176,177. Evacuation of stored sediment could depend heavily on the magnitude and duration of episodic events triggered by intense rainfall and extreme floods 75,188. Paraglaciation and mass wasting will dominate sediment supply and transport during stage III 120,176,192.

The timing of peak sediment (scenario B in Fig. 6) could occur in stage II under a stable precipitation scenario. The peak of sediment delivery may lag decades to hundreds of years behind peak meltwater, reflecting the increase in remobilization of paraglacial and subglacial sediment storage<sup>12,125,194</sup>; such a lag is likely to be scale-dependent, being shorter (years) close to the source region and much longer (decades to centuries) farther downstream<sup>194</sup>. With decreasing erosive rainfall, peak sediment could arrive earlier than peak meltwater (scenario A in Fig. 6), because increased accessibility to sediment supply would not compensate for reduced erosivity and transport capacity<sup>195</sup>. The increasing erosive rainfall could still constrain the peak sediment within stage II, accompanied by increased sediment yield and amplified variability through the remobilization of legacy sediment inherited from paraglacial environments<sup>19,188</sup> (scenario C in Fig. 6).

#### Challenges and complexity

Long-term field observations of erosion, sediment yield, and the environmental drivers of sediment fluxes are lacking in cold regions <sup>21,88,196,197</sup>, particularly for bedload and erosion rates. Access to the few available records is restricted by policy and technical barriers, and therefore little synthesis has been undertaken. Research biases probably exist — decreased sediment yield or reduced erosion could occur in some cryospheric basins, but few studies report such results <sup>68</sup>. Such limitations hamper the holistic assessment of geomorphic changes, spatiotemporal variations in sediment dynamics, and the response of basin-scale sediment yield to climate change <sup>21,88</sup>. The lack of field observations also impedes the development and application of sediment yield models, owing to the paucity of validation and calibration data and the poor parameterization of key geomorphic processes <sup>198,199</sup>.

Challenges and uncertainties in sediment-yield modelling and future projections also arise from the inherent complexity of geomorphic processes, characterized by scale effects on sediment transport<sup>199,200</sup>, episodic events<sup>201</sup>, nonlinear responses of geomorphic processes<sup>6,202</sup>, and climate feedbacks associated with cryosphere degradation<sup>203,204</sup>. Erosion and deposition processes vary across spatial scales, and the relative importance of factors controlling sediment dynamics are scale-dependent<sup>199,205</sup>. For example, climate, topography and catchment area can dominate global-scale variation of sediment yield<sup>206</sup>, but their influences on sediment yield can be obscured by local glacier dynamics, the extent of thermokarst landscapes, and sediment connectivity<sup>153,207,208</sup>.

Low-frequency and high-magnitude episodic sediment events (for example, mass wasting and GLOFs) can mobilize huge amounts of sediment during a short period, causing notable variability in both seasonal and annual sediment yields<sup>201</sup>. The frequency and duration of such extreme sediment events are difficult to predict<sup>3,88</sup>. Putting event data into a synthesis framework of 'geomorphic work', as proposed by Wolman and Miller in 1960, may shed light on this aspect of complexity<sup>209</sup>. However, another complication is that cryospheric regions generally owe their high altitude and steep topography to tectonic forces, and so seismically generated landslides and sediment

movement can confound detection of climate signals — examples of earthquake-generated landslides abound in the Himalaya, Alaska, New Zealand and the Andes  $^{16,94,210}$ .

Geomorphic responses to climate change can also be complicated by threshold effects, antecedent conditions and response time-lags<sup>21,202,211</sup>, thus precluding simulations by linear forcing-response models or universal constants<sup>6</sup>. Thresholds in geomorphic changes (for example, landslides) and related sediment mobilization can involve nonlinear and dynamic relationships between environmental drivers and geomorphic response<sup>212,213</sup>. Simulating such nonlinear and dynamic processes represents important challenges in Earth surface modelling, because of their spatiotemporal heterogeneity and sensitivity to the intrinsic properties of geomorphic systems and extrinsic drivers<sup>192,213</sup>, and the disproportionate amplification of geomorphic changes and sediment transport when thresholds are exceeded<sup>21,211</sup>.

Furthermore, melting and thawing of the cryosphere can amplify the atmospheric warming and affect the monsoon precipitation through feedback linked to permafrost carbon<sup>30</sup>, snow and ice albedo<sup>204</sup>, and land–sea temperature gradients<sup>214</sup>. These positive feedbacks add important uncertainties to climate model projections<sup>40,204</sup> and are likely to lead to underestimation when predicting future atmosphere warming, fluvial events and extreme sediment yields<sup>124,215</sup>.

In a warmer future, basin-scale sediment source-to-sink processes and sediment routing systems could be altered by spatial reorganization of sediment sources and/or sinks and river channels<sup>5,216</sup>, by changes in lateral and longitudinal connectivity<sup>153</sup>, by geomorphic feedbacks<sup>7</sup>, and by human activities<sup>27,217</sup> (Fig. 7). With glacier melt and permafrost thaw, rockfalls and landslides are likely to increase <sup>100,188</sup>. Increased slope failures could trigger GLOFs and temporarily convert glacial lakes from effective long-term sediment sinks into important sediment sources and transfer pathways, causing channel and valley erosion<sup>118</sup>.

In efficient, well-connected pristine sediment routing systems, intensified sediment transport leads to delta progradation<sup>4</sup> and increased terrestrial fluxes to the ocean (for example, Arctic deltas)<sup>218</sup> (Fig. 7). However, in most cases, only a small fraction of the sediment mobilized from mountain headwaters affected by cryosphere degradation will be transported downstream to basin outlets<sup>200</sup>, and the signals of climate-change-driven increases in sediment flux from the mountain erosion zone are attenuated by the buffering effects of floodplains and sediment sinks<sup>73,153</sup>. The concomitant processes of fluvial sorting, coarse sediment accumulation, and formation of debris fans can cause sediment disconnectivity<sup>7</sup> and buffer the downstream propagation of the sediment signal<sup>7,14</sup>. Increased human activity (for example, damming and sand mining) can also mute the signal of increased sediment loads from pristine uplands and even lead to delta subsidence<sup>217</sup>.

Long-term changes in the cryosphere and sediment fluxes can lead to river reorganization, change sediment delivery pathways and greatly alter downstream drainage networks (Fig. 7). However, the timing and intensity of river reorganization are affected by preconditions and the episodic nature of key triggers (Fig. 7). The upslope retreat of the Kaskawulsh Glacier in the Yukon redirected one headwater stream into another river in 2016, and this river piracy had far-reaching downstream hydrogeomorphic implications. Increased sediment deposition at mountain outlets in Himalayan, Andean and southwest New Zealand foreland basins has caused river avulsions and course-shifting during floods (75,219), redistributing the water and sediment on floodplains (11). The potential increases in river reorganization events in a warming future could further increase the uncertainty in large-scale sediment-yield predictions (75,220).

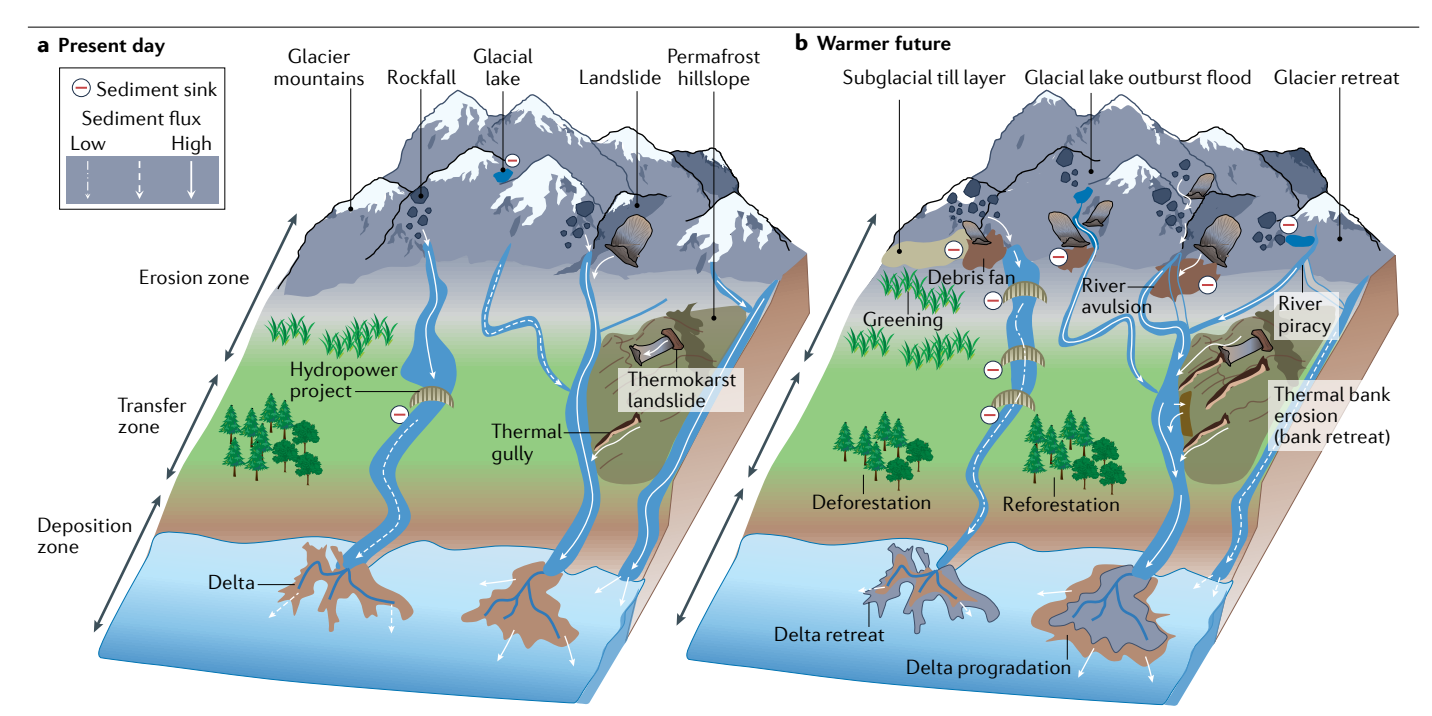


Fig. 7 | Changes in basin-scale sediment source-to-sink processes in response to climate change and human activities. The overall terrestrial sediment flux can be increased by sediment mobilization from retreated glaciers and thermokarst landscapes but decreased by the formation of natural and anthropogenic sediment sinks, with the net effect varying spatially.

 $\label{eq:approx} \textbf{a}, Present-day sediment source-to-sink processes. \textbf{b}, Sediment source-to-sink processes in a warmer future with intensified human activities. Vegetation change (for example, reforestation, deforestation and vegetation succession in proglacial areas) add uncertainties in estimating future changes in sediment yield.$ 

The impacts of landcover changes on sediment transport vary spatially <sup>221–223</sup>. Vegetation development in proglacial areas stabilizes slopes <sup>222</sup>, but this is also complicated by deglaciation-triggered slope instability and increases in erosive rainfall <sup>135,221</sup>. The overall greening in a warming Northern Hemisphere <sup>224</sup> and vegetation restoration in particular basins <sup>222,225</sup> contrast with local vegetation removal due to increased slope failures <sup>13,128,135</sup>. The net effect of landcover changes on sediment yield remains largely unknown.

#### **Summary and future perspectives**

Amplified atmospheric warming and the resulting melting and thawing of the cryosphere have markedly altered erosion and sediment delivery from the Earth's cryospheric basins<sup>1,4</sup>. The associated increased sediment yields have caused severe consequences for aquatic ecosystems, hazards and livelihoods<sup>21,22,175,180</sup>, but the public is still largely unprepared to deal with them. In this Review, we have compiled information on changing sediment fluxes from 76 locations (covering the high Arctic, European mountains, HMA and the Andes) with increased erosion (8) and sediment yields (68), and from 18 locations along Arctic coasts (Fig. 5). Increased sediment yields result from the increased glacier-bedrock erosion caused by increased meltwater and changes in basal sliding, the increased permafrost erosion caused by thermokarst landscape expansion, rock disintegration during deglaciation, and increases in sediment accessibility due to the exposure of underlying sediment stores and the initiation of new flow paths. However, the signal of sediment mobilization and transport can be moderated by increased sediment storage and reduced delivery efficacy due to the presence of sediment sinks, some of those (for example, hillslope-based debris fans) developing in response to increased erosion. Increases in sediment yield in most cryospheric basins are likely to continue in the next decades, with continued glacier melt and permafrost thaw, until the maximum sediment yield is reached. We posit that the timing of peak sediment is jointly regulated by changes in meltwater runoff, erosive rainfall and landscape erodibility (Fig. 7). To better assess the impacts of changing erosion and sediment yields on the functions and services of riverine and coastal ecosystems on the functions and services of riverine and coastal ecosystems, biogeochemical cycles the rerestrial—coastal landscape evolution and infrastructure systems, we highlight the pressing need to integrate multiple-sourced sediment observations, to develop physics-based sediment-transport models that include climatic feedbacks, and to promote interdisciplinary scientific collaboration.

Current understanding and assessment of the long-term response of erosion and sediment yields to climate-driven cryosphere changes remain incomplete. Sediment monitoring is lacking in most rivers (sediment loads are measured in <10% of the world's rivers)<sup>217</sup>, and decadal-scale sediment observations for cryospheric basins are even rarer<sup>2</sup>. Apart from expanding the traditional in situ sediment observations (for example, manual sediment sampling, automated sampling and turbidity monitoring)<sup>23,168</sup>, advances in remote sensing offer the opportunity to monitor sediment automatically and continuously and to reconstruct the temporal trends of erosion rates and sediment yields<sup>120</sup>. Breakthroughs in constraining relationships between surface reflectance and suspended-sediment concentration and extending retrieval algorithms worldwide beyond the calibration regions will

permit sediment information to be deciphered and extracted from previously unexploited satellite image archives, helping to fill the observation gaps <sup>31,226</sup> through making available more remote gauging stations <sup>227</sup>. The availability of satellite- and drone-observed images with a higher spatiotemporal resolution <sup>228</sup> and new techniques (for example, structure-from-motion photogrammetry) <sup>227</sup> will greatly improve the accuracy and precision of river pixels and further increase monitoring capabilities relating to sediment dynamics <sup>3,5,144,226</sup>. Optimization of calculating efficiency and access to the wide-ranging remotely sensed resources within the Google Earth engine will lead to near-real-time sediment monitoring <sup>227</sup>.

Ongoing developments in geochronology provide new approaches to obtain information from sediment. For example, lakes can record the long-term sedimentary history across decades to thousands of years 120,227 and this history can be reconstructed by using radioactive chronometers including caesium-137 (137Cs), radiocarbon (14C) and lead 210 (<sup>210</sup>Pb) to provide a chronology<sup>229</sup>. New technology in sediment-core collection and analysis will reveal the response of upstream watersediment dynamics and lake sedimentation to deglaciation<sup>173,230</sup>. Although cosmogenic nuclides (for example, beryllium-10, 10 Be) cannot reveal temporal changes in sediment yield owing to their long halflives, they can provide estimates of millennial-scale denudation rates and help in diagnosing the sediment sources 99,178. More investigations involving cosmogenic nuclide-derived millennial-scale denudation rates could provide a benchmark, thus underpinning the evaluation of current or future changes in denudation rates 99,120. Additionally, progress in environmental seismology can promote near-real-time sediment-transport and geomorphic analysis during extreme events such as GLOFs  $^{118,231}$  ; advances in sediment source fingerprinting can provide information on sediment sources to unravel the relative importance of different denudational processes<sup>112</sup>.

Physics-based sediment-yield models can offer valuable insights into past and future sediment dynamics in response to climate change and cryosphere degradation and can integrate sediment delivery processes into Earth System models to provide a better representation of land-ocean nutrient and carbon cycling. Existing sediment-yield models are mostly empirical or conceptual models (for example, SWAT, WBMsed<sup>232</sup>, HydroTrend<sup>233</sup>, BQART<sup>206</sup> and SAT<sup>8</sup>). Physics-based models are rare (for example, Water Erosion Prediction Project<sup>234</sup>) and only marginally account for the temperature-dependent erosional processes in cryospheric basins. A fully distributed physicsbased sediment-yield model that explicitly incorporates the various thermally and pluvially driven sediment mobilization and transport processes is urgently needed to simulate sediment yields from cryospheric basins at a high spatiotemporal resolution. Changes in both erosion and depositional sinks and associated changes in sediment connectivity<sup>14,132,153</sup> need to be considered in sediment-yield models, in order to evaluate the net effect of landscape changes in response to cryosphere degradation. By integrating deglaciation, thermokarst erosion, frost cracking and shifts in sediment-transport regimes, such models would advance the prediction of long-term sediment yields (including future systematic shifts in sediment mobilization and transport).

State-of-the-art geoscientific machine learning approaches offer an opportunity to address the challenges of data assimilation and spatiotemporal dynamics posed by the explosive growth of input data from multiple-sourced climate-cryosphere-hydrogeomorphology observations<sup>235,236</sup>. Additionally, coupling sediment-yield models with Earth System models would address constraints associated with

representing sediment-related carbon and nutrient dynamics at large scales and better capture biogeochemical cycles and their feedbacks<sup>237</sup>.

To advance a holistic understanding of sediment dynamics in the world's cold environments, the innovative system approach would best come from the creation of an interdisciplinary collaborative initiative, where climatologists, ecologists, glaciologists, permafrost scientists, hydrologists, civil engineers and geomorphologists work together to establish an integrated cryosphere–water–sediment–environment observation platform that facilitates the development of fully distributed physics-based sediment-yield models. Furthermore, dialogues and collaboration between international scientists, stakeholders, local communities, and policymakers would help to bridge the gaps between state-of-the-art scientific findings and practicable adaptation strategies. Such collaboration and dialogues would help to address climate-change-driven sediment issues and problems and aid the establishment of sustainable and climate-resilient infrastructure systems and riparian and coastal ecosystems in strategically important cold regions.

#### **Data availability**

The warming-driven changes in erosion and sediment yield inventory is available at: https://zenodo.org/record/7109898.

Published online: 1 November 2022

#### References

- Li, D. et al. Exceptional increases in fluvial sediment fluxes in a warmer and wetter High Mountain Asia. Science 374, 599-603 (2021).
- Syvitski, J. et al. Earth's sediment cycle during the Anthropocene. Nat. Rev. Earth Environ. https://doi.org/10.1038/s43017-021-00253-w (2022).
- Lewkowicz, A. G. & Way, R. G. Extremes of summer climate trigger thousands of thermokarst landslides in a high Arctic environment. Nat. Commun. 10, 1329 (2019).
- Bendixen, M. et al. Delta progradation in Greenland driven by increasing glacial mass loss. Nature 550, 101–104 (2017).
- Shugar, D. H. et al. River piracy and drainage basin reorganization led by climate-driven glacier retreat. Nat. Geosci. 10, 370–375 (2017).
- Knight, J. & Harrison, S. The impacts of climate change on terrestrial Earth surface systems. Nat. Clim. Change 3, 24–29 (2012).
- Lane, S. N., Bakker, M., Gabbud, C., Micheletti, N. & Saugy, J.-N. Sediment export, transient landscape response and catchment-scale connectivity following rapid climate warming and alpine glacier recession. Geomo 277, 210–227 (2017).
- Zhang, T., Li, D., Kettner, A. J., Zhou, Y. & Lu, X. Constraining dynamic sediment-discharge relationships in cold environments: the sediment-availability-transport (SAT) model. Water Resour. Res. https://doi.org/10.1029/2021wr030690 (2021).
- 9. Herman, F. et al. Erosion by an alpine glacier. Science 350, 193-195 (2015).
- Lane, S. N. & Nienow, P. W. Decadal-scale climate forcing of alpine glacial hydrological systems. Water Resour. Res. 55, 2478–2492 (2019).
- Huss, M. & Hock, R. Global-scale hydrological response to future glacier mass loss. Nat. Clim. Change 8, 135–140 (2018).
- Delaney, I. & Adhikari, S. Increased subglacial sediment discharge in a warming climate: consideration of ice dynamics, glacial erosion, and fluvial sediment transport. Geophys. Res. Lett. https://doi.org/10.1029/2019gl085672 (2020).
- Li, D., Overeem, I., Kettner, A. J., Zhou, Y. & Lu, X. Air temperature regulates erodible landscape, water, and sediment fluxes in the permafrost-dominated catchment on the Tibetan Plateau. Water Resour. Res. 57, e2020WR028193 (2021).
- Mancini, D. & Lane, S. N. Changes in sediment connectivity following glacial debuttressing in an alpine valley system. Geomo https://doi.org/10.1016/j.geomorph. 2019.106987 (2020).
- Koppes, M. et al. Observed latitudinal variations in erosion as a function of glacier dynamics. Nature 526, 100–103 (2015).
- Kirschbaum, D., Kapnick, S. B., Stanley, T. & Pascale, S. Changes in extreme precipitation and landslides over High Mountain Asia. Geophys. Res. Lett. 47, e2019GL085347 (2020).
- Patton, A. I., Rathburn, S. L., Capps, D. M., McGrath, D. & Brown, R. A. Ongoing landslide deformation in thawing permafrost. Geophys. Res. Lett. https://doi.org/10.1029/ 2021gl092959 (2021).
- Syvitski, J. P. M. Sediment discharge variability in Arctic rivers: implications for a warmer future. Polar Res. 21, 323–330 (2002).
- Beel, C. R. et al. Emerging dominance of summer rainfall driving high Arctic terrestrialaquatic connectivity. Nat. Commun. 12, 1448 (2021).
- Patton, A. I., Rathburn, S. L. & Capps, D. M. Landslide response to climate change in permafrost regions. Geomo 340, 116–128 (2019).

- East, A. E. & Sankey, J. B. Geomorphic and sedimentary effects of modern climate change: current and anticipated future conditions in the western United States. Rev. Geophys. https://doi.org/10.1029/2019rg000692 (2020).
- Li, D. et al. High Mountain Asia hydropower systems threatened by climate-driven landscape instability. Nat. Geosci. https://doi.org/10.1038/s41561-022-00953-y (2022).
- Vergara, I., Garreaud, R. & Ayala, Á. Sharp increase of extreme turbidity events due to deglaciation in the subtropical Andes. J. Geophys. Res. Earth Surf. https://doi.org/ 10.1029/2021jf006584 (2022).
- Hopwood, M. J. et al. Non-linear response of summertime marine productivity to increased meltwater discharge around Greenland. Nat. Commun. 9, 3256 (2018).
- Yi, Y., Liu, Q., Zhang, J. & Zhang, S. How do the variations of water and sediment fluxes into the estuary influence the ecosystem? J. Hydrol. https://doi.org/10.1016/ j.jhydrol.2021.126523 (2021).
- Immerzeel, W. W. et al. Importance and vulnerability of the world's water towers. Nature 577, 364–369 (2020)
- 27. Best, J. Anthropogenic stresses on the world's big rivers. Nat. Geosci. 12, 7-21 (2019).
- Li, X. et al. Globally elevated chemical weathering rates beneath glaciers. Nat. Commun. https://doi.org/10.1038/s41467-022-28032-1 (2022).
- Hilton, R. G. & West, A. J. Mountains, erosion and the carbon cycle. Nat. Rev. Earth Environ. 1, 284–299 (2020).
- Turetsky, M. R. et al. Carbon release through abrupt permafrost thaw. Nat. Geosci. 13, 138–143 (2020).
- Overeem, I. et al. Substantial export of suspended sediment to the global oceans from glacial erosion in Greenland. Nat. Geosci. 10, 859–863 (2017).
- 32. Arrigo, K. R. et al. Melting glaciers stimulate large summer phytoplankton blooms in southwest Greenland waters. *Geophys. Res. Lett.* **44**, 6278–6285 (2017).
- Lantuit, H. et al. The Arctic coastal dynamics database: a new classification scheme and statistics on Arctic permafrost coastlines. Estuaries Coast. 35, 383–400 (2012).
- Hjort, J. et al. Degrading permafrost puts Arctic infrastructure at risk by mid-century. Nat. Commun. 9, 5147 (2018).
- Wild, B. et al. Rivers across the Siberian Arctic unearth the patterns of carbon release from thawing permafrost. Proc. Natl Acad. Sci. USA 116, 10280–10285 (2019).
- Micheletti, N. & Lane, S. N. Water yield and sediment export in small, partially glaciated alpine watersheds in a warming climate. Water Resour. Res. 52, 4924–4943 (2016).
- Beel, C. R. et al. Differential impact of thermal and physical permafrost disturbances on high Arctic dissolved and particulate fluvial fluxes. Sci. Rep. 10, 11836 (2020).
- Shugar, D. H. et al. A massive rock and ice avalanche caused the 2021 disaster at Chamoli. Indian Himalava. Science 373. 300–306 (2021).
- Farinotti, D., Immerzeel, W. W., de Kok, R., Quincey, D. J. & Dehecq, A. Manifestations and mechanisms of the Karakoram glacier anomaly. *Nat. Geosci.* 13, 8–16 (2020).
- Hock, R. G. et al. in Special Report on the Ocean and Cryosphere in a Changing Climate (eds Portner, H.-O. et al.) 181–202 (IPCC, Cambridge Univ. Press, 2019).
- Zemp, M. et al. Global glacier mass changes and their contributions to sea-level rise from 1961 to 2016. Nature 558, 382–386 (2019).
- Hugonnet, R. et al. Accelerated global glacier mass loss in the early twenty-first century. Nature 592, 726-731 (2021).
- Hock, R. et al. GlacierMIP-a model intercomparison of global-scale glacier mass-balance models and projections. J. Glaciol. 65, 453-467 (2019).
- Marzeion, B. et al. Partitioning the uncertainty of ensemble projections of global glacier mass change. Earths Future https://doi.org/10.1029/2019ef001470 (2020).
- Huss, M. & Hock, R. A new model for global glacier change and sea-level rise. Front. Earth Sci. https://doi.org/10.3389/feart.2015.00054 (2015).
- Ciraci, E., Velicogna, I. & Swenson, S. Continuity of the mass loss of the world's glaciers and ice caps from the GRACE and GRACE follow-on missions. Geophys. Res. Lett. https://doi.org/10.1029/2019gl086926 (2020).
- Truffer, M., Motyka, R. J., Hekkers, M., Howat, I. M. & King, M. A. Terminus dynamics at an advancing glacier: Taku Glacier, Alaska. J. Glaciol. 55, 1052-1060 (2009).
- Shugar, D. H. et al. Rapid worldwide growth of glacial lakes since 1990. Nat. Clim. Change 10, 939–945 (2020).
- Carrivick, J. L. & Tweed, F. S. A global assessment of the societal impacts of glacier outburst floods. Glob. Planet. Change 144, 1–16 (2016).
- Veh, G. et al. Trends, breaks, and biases in the frequency of reported glacier lake outburst floods. Earths Future https://doi.org/10.1029/2021ef002426 (2022).
- Li, X. et al. Climate change threatens terrestrial water storage over the Tibetan Plateau. Nat. Clim. Change https://doi.org/10.1038/s41558-022-01443-0 (2022).
- 52. Biskaborn, B. K. et al. Permafrost is warming at a global scale. Nat. Commun. 10, 264 (2019).
- Gruber, S. et al. Inferring permafrost and permafrost thaw in the mountains of the Hindu Kush Himalaya region. Cryosphere 11, 81–99 (2017).
- Smith, S. L., O'Neill, H. B., Isaksen, K., Noetzli, J. & Romanovsky, V. E. The changing thermal state of permafrost. Nat. Rev. Earth Environ. 3, 10–23 (2022).
- Chadburn, S. E. et al. An observation-based constraint on permafrost loss as a function of global warming. Nat. Clim. Change 7, 340–344 (2017).
- Overeem, I. et al. A modeling toolbox for permafrost landscapes. EOS Trans. Am. Geophys. Un. https://doi.org/10.1029/2018EO105155 (2018).
- Farquharson, L. M. et al. Climate change drives widespread and rapid thermokarst development in very cold permafrost in the Canadian high Arctic. Geophys. Res. Lett. 46, 6681–6689 (2019).
- Veremeeva, A., Nitze, I., Günther, F., Grosse, G. & Rivkina, E. Geomorphological and climatic drivers of thermokarst lake area increase trend (1999–2018) in the Kolyma

- Lowland Yedoma region, north-eastern Siberia. Remote Sens. https://doi.org/10.3390/rs13020178 (2021).
- Segal, R. A., Lantz, T. C. & Kokelj, S. V. Acceleration of thaw slump activity in glaciated landscapes of the western Canadian Arctic. *Environ. Res. Lett.* https://doi.org/10.1088/ 1748-9326/11/3/034025 (2016).
- Mu, C. et al. Acceleration of thaw slump during 1997–2017 in the Qilian Mountains of the northern Qinghai-Tibetan Plateau. *Landslides* 17, 1051–1062 (2020).
- Hjort, J. et al. Impacts of permafrost degradation on infrastructure. Nat. Rev. Earth Environ. 3, 24–38 (2022).
- 62. Olefeldt, D. et al. Circumpolar distribution and carbon storage of thermokarst landscapes. *Nat. Commun.* **7**, 13043 (2016).
- Kanevskiy, M. et al. Patterns and rates of riverbank erosion involving ice-rich permafrost (yedoma) in northern Alaska. Geomo 253, 370–384 (2016).
- Jones, B. M. et al. Lake and drained lake basin systems in lowland permafrost regions. Nat. Rev. Earth Environ. 3, 85–98 (2022).
- Kokelj, S. V., Lantz, T. C., Tunnicliffe, J., Segal, R. & Lacelle, D. Climate-driven thaw of permafrost preserved glacial landscapes, northwestern Canada. Geology 45, 371–374 (2017).
- Cheng, G. et al. Characteristic, changes and impacts of permafrost on Qinghai-Tibet Plateau. Chin. Sci. Bull. 64, 2783–2795 (2019).
- Luo, J., Niu, F., Lin, Z., Liu, M. & Yin, G. Recent acceleration of thaw slumping in permafrost terrain of Qinghai-Tibet Plateau: an example from the Beiluhe region. Geomorphology 341, 79–85 (2019).
- Irrgang, A. M. et al. Drivers, dynamics and impacts of changing Arctic coasts. Nat. Rev. Earth Environ. 3, 39–54 (2022).
- Pörtner, H.-O. et al. The ocean and cryosphere in a changing climate. Special Report on the Ocean and Cryosphere in a Changing Climate (eds Pörtner, H.-O. et al.) (IPCC, Cambridge Univ. Press, 2019).
- Barnhart, K. R., Miller, C. R., Overeem, I. & Kay, J. E. Mapping the future expansion of Arctic open water. Nat. Clim. Change 6, 280–285 (2015).
- Maslakov, A. & Kraev, G. Erodibility of permafrost exposures in the coasts of Eastern Chukotka. Polar Sci. 10, 374–381 (2016).
- Jones, B. M. et al. A decade of remotely sensed observations highlight complex processes linked to coastal permafrost bluff erosion in the Arctic. Environ. Res. Lett. https://doi.org/10.1088/1748-9326/aae471 (2018).
- Jaeger, J. M. & Koppes, M. N. The role of the cryosphere in source-to-sink systems. Earth Sci. Rev. 153, 43–76 (2016).
- 74. Herman, F., De Doncker, F., Delaney, I., Prasicek, G. & Koppes, M. The impact of glaciers on mountain erosion. *Nat. Rev. Earth Environ.* **2**, 422–435 (2021).
- Antoniazza, G. & Lane, S. N. Sediment yield over glacial cycles: a conceptual model. Prog. Phys. Geogr. Earth Environ. https://doi.org/10.1177/0309133321997292 (2021).
- Hallet, B., Hunter, L. & Bogen, J. Rates of erosion and sediment evacuation by glaciers: a review of field data and their implications. Glob. Planet. Change 12, 213–235 (1996).
- Cook, S. J., Swift, D. A., Kirkbride, M. P., Knight, P. G. & Waller, R. I. The empirical basis for modelling glacial erosion rates. *Nat. Commun.* 11, 759 (2020).
- Ugelvig, S. V., Egholm, D. L., Anderson, R. S. & Iverson, N. R. Glacial erosion driven by variations in meltwater drainage. J. Geophys. Res. Earth Surf. 123, 2863–2877 (2018).
- Iverson, N. R. A theory of glacial quarrying for landscape evolution models. Geology 40, 679–682 (2012).
- 80. Hallet, B. Glacial quarrying: a simple theoretical model. Ann. Glaciol. 22, 1–8 (1996).
- 81. Dühnforth, M., Anderson, R. S., Ward, D. & Stock, G. M. Bedrock fracture control of glacial erosion processes and rates. Geology **38**, 423–426 (2010).
- 82. Bernard, H. A theoretical model of glacial abrasion. J. Glaciol. 23, 39-50 (1979).
- Iverson, N. R. Laboratory simulations of glacial abrasion: comparison with theory. J. Glaciol. 36, 304–314 (1990).
- 84. Harbor, J. M., Hallet, B. & Raymond, C. F. A numerical model of landform development by glacial erosion. *Nature* **333**, 347–349 (1988).
- MacGregor, J. A. et al. A synthesis of the basal thermal state of the Greenland ice sheet. J. Geophys. Res. Earth Surf. 121, 1328-1350 (2016).
- Dehecq, A. et al. Twenty-first century glacier slowdown driven by mass loss in High Mountain Asia. Nat. Geosci. 12, 22–27 (2018).
- Phillips, T., Rajaram, H. & Steffen, K. Cryo-hydrologic warming: a potential mechanism for rapid thermal response of ice sheets. Geophys. Res. Lett. https://doi.org/10.1029/ 2010gl044397 (2010).
- Carrivick, J. L. & Tweed, F. S. Deglaciation controls on sediment yield: towards capturing spatio-temporal variability. *Earth Sci. Rev.* https://doi.org/10.1016/j.earscirev.2021.103809 (2021).
- Herman, F., Beaud, F., Champagnac, J.-D., Lemieux, J.-M. & Sternai, P. Glacial hydrology and erosion patterns: a mechanism for carving glacial valleys. *Earth Planet. Sci. Lett.* 310, 498–508 (2011).
- Alley, R. B. et al. How glaciers entrain and transport basal sediment: physical constraints. Quat. Sci. Rev. 16, 1017–1038 (1997).
- Hartmeyer, I. et al. Current glacier recession causes significant rockfall increase: the immediate paraglacial response of deglaciating cirque walls. Earth Surf. Dyn. 8, 729–751 (2020).
- Coe, J. A., Bessette-Kirton, E. K. & Geertsema, M. Increasing rock-avalanche size and mobility in Glacier Bay National Park and Preserve, Alaska detected from 1984 to 2016 Landsat imagery. *Landslides* 15, 393–407 (2017).

- Beylich, A. A. & Laute, K. Sediment sources, spatiotemporal variability and rates of fluvial bedload transport in glacier-connected steep mountain valleys in western Norway (Erdalen and Bødalen drainage basins). Geomorphology 228, 552–567 (2015).
- Allen, S. K., Cox, S. C. & Owens, I. F. Rock avalanches and other landslides in the central Southern Alps of New Zealand: a regional study considering possible climate change impacts. *Landslides* 8, 33–48 (2010).
- Chiarle, M., Geertsema, M., Mortara, G. & Clague, J. J. Relations between climate change and mass movement: perspectives from the Canadian Cordillera and the European Alps. Glob. Planet. Change https://doi.org/10.1016/j.gloplacha.2021.103499 (2021).
- Matsuoka, N. Frost weathering and rockwall erosion in the southeastern Swiss Alps: long-term (1994–2006) observations. Geomorphology 99, 353–368 (2008).
- Murton, J. B., Peterson, R. & Ozouf, J.-C. Bedrock fracture by ice segregation in cold regions. Science 314, 1127–1129 (2006).
- Kellerer-Pirklbauer, A. Potential weathering by freeze-thaw action in alpine rocks in the European Alps during a nine year monitoring period. Geomorphology 296, 113–131 (2017).
- Scherler, D. & Egholm, D. L. Production and transport of supraglacial debris: insights from cosmogenic <sup>10</sup>Be and numerical modeling, Chhota Shigri Glacier, Indian Himalaya. J. Geophys. Res. Earth Surf. https://doi.org/10.1029/2020if005586 (2020).
- 100. Evans, S. G. & Delaney, K. B. in *Snow and Ice-Related Hazards, Risks, and Disasters* (eds Shroder, J. F., Haeberli, W. & Whiteman, C.) 563–606 (Academic, 2015).
- Beaud, F., Flowers, G. E. & Venditti, J. G. Efficacy of bedrock erosion by subglacial water flow. Earth Surf. Dyn. 4, 125–145 (2016).
- Gimbert, F., Tsai, V. C., Amundson, J. M., Bartholomaus, T. C. & Walter, J. I. Subseasonal changes observed in subglacial channel pressure, size, and sediment transport. Geophys. Res. Lett. 43, 3786–3794 (2016).
- 103. Swift, D. A. et al. The hydrology of glacier-bed overdeepenings: sediment transport mechanics, drainage system morphology, and geomorphological implications. *Earth Surf. Process. Landforms* 46, 2264–2278 (2021).
- Andrews, L. C. et al. Direct observations of evolving subglacial drainage beneath the Greenland ice sheet. Nature 514, 80–83 (2014).
- Colgan, W. et al. An increase in crevasse extent, West Greenland: hydrologic implications. Geophys. Res. Lett. https://doi.org/10.1029/2011gl048491 (2011).
- Nienow, P., Sharp, M. & Willis, I. Seasonal changes in the morphology of the subglacial drainage system, Haut Glacier d'Arolla, Switzerland. Earth Surf. Process. Landforms 23, 825–843 (1998).
- Chudley, T. R. et al. Supraglacial lake drainage at a fast-flowing Greenlandic outlet glacier. Proc. Natl Acad. Sci. USA 116, 25468–25477 (2019).
- Smith, L. C. et al. Efficient meltwater drainage through supraglacial streams and rivers on the southwest Greenland ice sheet. Proc. Natl Acad. Sci. USA 112, 1001–1006 (2015).
- Livingstone, S. J. et al. Subglacial lakes and their changing role in a warming climate Nat. Rev. Earth Environ. https://doi.org/10.1038/s43017-021-00246-9 (2022).
- Livingstone, S. J. et al. Brief communication: subglacial lake drainage beneath Isunguata Sermia, West Greenland: geomorphic and ice dynamic effects. Cryosphere 13, 2789–2796 (2019).
- Gabet, E., Burbank, D., Prattsitaula, B., Putkonen, J. & Bookhagen, B. Modern erosion rates in the High Himalayas of Nepal. Earth Planet. Sci. Lett. 267, 482–494 (2008).
- Tsyplenkov, A., Vanmaercke, M., Collins, A. L., Kharchenko, S. & Golosov, V. Elucidating suspended sediment dynamics in a glacierized catchment after an exceptional erosion event: the Djankuat catchment, Caucasus Mountains, Russia. Catena https://doi.org/ 10.1016/j.catena.2021.105285 (2021).
- Beylich, A. A., Laute, K. & Storms, J. E. A. Contemporary suspended sediment dynamics within two partly glacierized mountain drainage basins in western Norway (Erdalen and Bødalen, inner Nordfjord). Geomorphology 287, 126–143 (2017).
- Comiti, F. et al. Glacier melt runoff controls bedload transport in alpine catchments. Earth Planet. Sci. Lett. 520, 77–86 (2019).
- Williams, H. B. & Koppes, M. N. A comparison of glacial and paraglacial denudation responses to rapid glacial retreat. Ann. Glaciol. 60, 151–164 (2019).
- Bogen, J., Xu, M. & Kennie, P. The impact of pro-glacial lakes on downstream sediment delivery in Norway. Earth Surf. Process. Landforms 40, 942–952 (2014).
- Steffen, T., Huss, M., Estermann, R., Hodel, E. & Farinotti, D. Volume, evolution, and sedimentation of future glacier lakes in Switzerland over the 21st century. *Earth Surf. Dyn.* 10, 723–741 (2022).
- Cook, K. L., Andermann, C., Gimbert, F., Adhikari, B. R. & Hovius, N. Glacial lake outburst floods as drivers of fluvial erosion in the Himalaya. Science 362, 53–57 (2018).
- Cenderelli, D. A. & Wohl, E. E. Flow hydraulics and geomorphic effects of glacial-lake outburst floods in the Mount Everest region, Nepal. Earth Surf. Process. Landforms 28, 385–407 (2003).
- Heckmann, T., McColl, S. & Morche, D. Retreating ice: research in pro-glacial areas matters. Earth Surf. Process. Landforms 41, 271–276 (2016).
- Tomczyk, A. M., Ewertowski, M. W. & Carrivick, J. L. Geomorphological impacts of a glacier lake outburst flood in the high Arctic Zackenberg River, NE Greenland. J. Hydrol. https://doi.org/10.1016/i.ihydrol.2020.125300 (2020).
- Russell, A. J. et al. Icelandic jökulhlaup impacts: implications for ice-sheet hydrology, sediment transfer and geomorphology. Geomorphology 75, 33–64 (2006).
- Wilson, R. et al. The 2015 Chileno Valley glacial lake outburst flood, Patagonia. Geomorphology 332, 51–65 (2019).
- IPCC Climate Change 2021: The Physical Science Basis (eds Masson-Delmotte, V. et al.) (Cambridge Univ. Press, 2021).

- de Winter, I. L., Storms, J. E. A. & Overeem, I. Numerical modeling of glacial sediment production and transport during deglaciation. Geomorphology 167-168, 102-114 (2012).
- 126. Lai, J. & Anders, A. M. Climatic controls on mountain glacier basal thermal regimes dictate spatial patterns of glacial erosion. *Earth Surf. Dyn.* **9**, 845–859 (2021).
- Hirschberg, J. et al. Climate change impacts on sediment yield and debris-flow activity in an alpine catchment. J. Geophys. Res. Earth Surf. 126, e2020JF005739 (2021).
- Kokelj, S. V. et al. Thawing of massive ground ice in mega slumps drives increases in stream sediment and solute flux across a range of watershed scales. J. Geophys. Res. Earth Surf. 118, 681–692 (2013).
- Rudy, A. C. A., Lamoureux, S. F., Kokelj, S. V., Smith, I. R. & England, J. H. Accelerating thermokarst transforms ice-cored terrain triggering a downstream cascade to the ocean. Geophys. Res. Lett. https://doi.org/10.1002/2017q1074912 (2017).
- Lafrenière, M. J. & Lamoureux, S. F. Effects of changing permafrost conditions on hydrological processes and fluvial fluxes. Earth Sci. Rev. 191, 212–223 (2019).
- Lamoureux, S. F., Lafrenière, M. J. & Favaro, E. A. Erosion dynamics following localized permafrost slope disturbances. Geophys. Res. Lett. 41, 5499–5505 (2014).
- 132. Godin, E., Fortier, D. & Coulombe, S. Effects of thermo-erosion gullying on hydrologic flow networks, discharge and soil loss. *Environ. Res. Lett.* **9**, 105010 (2014).
- Obu, J. et al. Effect of terrain characteristics on soil organic carbon and total nitrogen stocks in soils of Herschel Island, Western Canadian Arctic. Permafr. Periglac. Process 28, 92–107 (2017).
- Lewkowicz, A. G. Dynamics of active-layer detachment failures, Fosheim Peninsula, Ellesmere Island, Nunavut, Canada. Permafr. Periglac. Process. 18, 89-103 (2007).
- Gooseff, M. N., Balser, A., Bowden, W. B. & Jones, J. B. Effects of hillslope thermokarst in Northern Alaska. Eos, Trans. Am. Geophys. Union. 90, 29–30 (2009).
- Paquette, M., Rudy, A. C. A., Fortier, D. & Lamoureux, S. F. Multi-scale site evaluation of a relict active layer detachment in a high Arctic landscape. Geomorphology https:// doi.org/10.1016/j.geomorph.2020.107159 (2020).
- Balser, A. W., Jones, J. B. & Gens, R. Timing of retrogressive thaw slump initiation in the Noatak Basin, northwest Alaska, USA. J. Geophys. Res. Earth Surf. 119, 1106–1120 (2014).
- Godin, E. & Fortier, D. Geomorphology of a thermo-erosion gully, Bylot Island, Nunavut, Canada. Can. J. Earth Sci. 49, 979–986 (2012).
- Perreault, N., Lévesque, E., Fortier, D., Gratton, D. & Lamarque, L. J. Remote sensing evaluation of high Arctic wetland depletion following permafrost disturbance by thermo-erosion gullying processes. Arct. Sci. 3, 237–253 (2017).
- Kokelj, S. V. et al. Thaw-driven mass wasting couples slopes with downstream systems, and
  effects propagate through Arctic drainage networks. Cryosphere 15, 3059–3081 (2021).
- Zheng, L., Overeem, I., Wang, K. & Clow, G. D. Changing Arctic river dynamics cause localized permafrost thaw. J. Geophys. Res. Earth Surf. 124, 2324–2344 (2019).
- Lantuit, H. & Pollard, W. H. Fifty years of coastal erosion and retrogressive thaw slump activity on Herschel Island, southern Beaufort Sea, Yukon Territory, Canada. Geomorphology 95, 84–102 (2008).
- Costard, F., Dupeyrat, L., Gautier, E. & Carey-Gailhardis, E. Fluvial thermal erosion investigations along a rapidly eroding river bank: application to the Lena River (central Siberia). Earth Surf. Process. Landforms 28, 1349–1359 (2003).
- Payne, C., Panda, S. & Prakash, A. Remote sensing of river erosion on the Colville River, North Slope Alaska. Remote Sens. https://doi.org/10.3390/rs10030397 (2018).
- Costard, F. et al. Impact of the global warming on the fluvial thermal erosion over the Lena River in Central Siberia. Geophys. Res. Lett. https://doi.org/10.1029/2007gl030212 (2007).
- 146. Gautier, E. et al. Fifty-year dynamics of the Lena River islands (Russia): spatio-temporal pattern of large periglacial anabranching river and influence of climate change. Sci. Total Environ. 783, 147020 (2021).
- Shur, Y. et al. Fluvio-thermal erosion and thermal denudation in the yedoma region of northern Alaska: revisiting the Itkillik River exposure. Permafr. Periglac. Process. 32, 277–298 (2021).
- Chassiot, L., Lajeunesse, P. & Bernier, J.-F. Riverbank erosion in cold environments: review and outlook. Earth Sci. Rev. https://doi.org/10.1016/j.earscirev.2020.103231 (2020).
- Vandermause, R., Harvey, M., Zevenbergen, L. & Ettema, R. River-ice effects on bank erosion along the middle segment of the Susitna River, Alaska. Cold Reg. Sci. Technol. https://doi.org/10.1016/j.coldregions.2021.103239 (2021).
- Costard, F., Gautier, E., Fedorov, A., Konstantinov, P. & Dupeyrat, L. An assessment of the erosion potential of the fluvial thermal process during ice breakups of the Lena River (Siberia). Permafr. Periglac. Process. 25, 162–171 (2014).
- Beltaos, S., Carter, T., Rowsell, R. & DePalma, S. G. S. Erosion potential of dynamic ice breakup in Lower Athabasca River. Part I: field measurements and initial quantification. Cold Reg. Sci. Technol. 149, 16–28 (2018).
- Rowland, J. C. et al. Arctic landscapes in transition: responses to thawing permafrost. Eos Trans. Am. Geophys. Union. 91, 229–230 (2010).
- 153. Wohl, E. et al. Connectivity as an emergent property of geomorphic systems. Earth Surf. Process. Landforms 44, 4–26 (2019).
  154. Walvoord, M. A. & Kurylyk, B. L. Hydrologic impacts of thawing permafrost a review.
- Vadose Zone J. **15**, 1–20 (2016). 155. Zhang, T., Li, D. & Lu, X. Response of runoff components to climate change in the source-
- region of the Yellow River on the Tibetan plateau. *Hydrol. Process.* https://doi.org/10.1002/hyp.14633 (2022). 156. Farquharson, L. M., Romanovsky, V. E., Kholodov, A. & Nicolsky, D. Sub-aerial talik
- Farquharson, L. M., Romanovsky, V. E., Kholodov, A. & Nicolsky, D. Sub-aerial talik formation observed across the discontinuous permafrost zone of Alaska. *Nat. Geosci.* 15, 475–481 (2022).

- Nitzbon, J. et al. Fast response of cold ice-rich permafrost in northeast Siberia to a warming climate. Nat. Commun. 11, 2201 (2020).
- Jones, B. M. et al. Arctic Report Card 2020: Coastal Permafrost Erosion. https://doi.org/ 10.25923/e47w-dw52 (NOAA Institutional Repository, 2020).
- 159. Günther, F., Overduin, P. P., Sandakov, A. V., Grosse, G. & Grigoriev, M. N. Short- and long-term thermo-erosion of ice-rich permafrost coasts in the Laptev Sea region. Biogeosciences 10, 4297–4318 (2013).
- Lim, M. et al. Massive ice control on permafrost coast erosion and sensitivity. Geophys. Res. Lett. https://doi.org/10.1029/2020g1087917 (2020).
- Frederick, J. M., Thomas, M. A., Bull, D. L., Jones, C. A. & Roberts, J. D. The Arctic Coastal Erosion Problem. Sandia Report No. SAND2016-9762 (Sandia National Laboratories, 2016).
- Overeem, I. et al. Sea ice loss enhances wave action at the Arctic coast. Geophys. Res. Lett. 38, L17503 (2011).
- 163. Radosavljevic, B. et al. Erosion and flooding threats to coastal infrastructure in the arctic: a case study from Herschel Island, Yukon Territory, Canada. Estuaries Coasts 39, 900–915 (2015).
- 164. Couture, N. J., Irrgang, A., Pollard, W., Lantuit, H. & Fritz, M. Coastal erosion of permafrost soils along the Yukon coastal plain and fluxes of organic carbon to the Canadian Beaufort Sea. J. Geophys. Res. Biogeosci. 123, 406–422 (2018).
- Delaney, I., Bauder, A., Werder, M. A. & Farinotti, D. Regional and annual variability in subglacial sediment transport by water for two glaciers in the Swiss Alps. Front. Earth Sci. https://doi.org/10.3389/feart.2018.00175 (2018).
- Comte, J., Monier, A., Crevecoeur, S., Lovejoy, C. & Vincent, W. F. Microbial biogeography of permafrost thaw ponds across the changing northern landscape. *Ecography* 39, 609–618 (2016).
- Fuchs, M. et al. Rapid fluvio-thermal erosion of a Yedoma permafrost cliff in the Lena River delta. Front. Earth Sci. https://doi.org/10.3389/feart.2020.00336 (2020).
- 168. Li, D., Li, Z., Zhou, Y. & Lu, X. Substantial increases in the water and sediment fluxes in the headwater region of the Tibetan Plateau in response to global warming. Geophys. Res. Lett. 47, e2020GL087745 (2020).
- Zhang, F. et al. Controls on seasonal erosion behavior and potential increase in sediment evacuation in the warming Tibetan Plateau. Catena https://doi.org/10.1016/j.catena. 2021.105797 (2022).
- Singh, A. et al. Counter-intuitive influence of Himalayan river morphodynamics on Indus Civilisation urban settlements. Nat. Commun. 8, 1617 (2017).
- Gabbud, C., Robinson, C. T. & Lane, S. N. Summer is in winter: disturbance-driven shifts in macroinvertebrate communities following hydroelectric power exploitation. Sci. Total Environ. 650, 2164–2180 (2019).
- Fischer, L., Huggel, C., Kääb, A. & Haeberli, W. Slope failures and erosion rates on a glacierized high-mountain face under climatic changes. *Earth Surf. Process. Landforms* 38, 836–846 (2013).
- Bogen, J. The impact of climate change on glacial sediment delivery to rivers. IAHS Publ. 325, 432-439 (2008).
- Singh, A. T. et al. Water discharge and suspended sediment dynamics in the Chandra River, Western Himalaya. J. Earth Syst. Sci. https://doi.org/10.1007/s12040-020-01455-4 (2020).
- 175. Brooke, S. et al. Where rivers jump course. Science 376, 987-990 (2022).
- Church, M. & Ryder, J. M. Paraglacial sedimentation: a consideration of fluvial processes conditioned by glaciation. GSA Bull. 83, 3059–3072 (1972).
- 177. Ballantyne, C. K. Paraglacial geomorphology. Quat. Sci. Rev. 21, 1935–2017 (2002).
- Mariotti, A. et al. Nonlinear forcing of climate on mountain denudation during glaciations. Nat. Geosci. https://doi.org/10.1038/s41561-020-00672-2 (2021).
- Moon, S. et al. Climatic control of denudation in the deglaciated landscape of the Washington Cascades. Nat. Geosci. 4, 469–473 (2011).
- Terhaar, J., Lauerwald, R., Regnier, P., Gruber, N. & Bopp, L. Around one third of current Arctic Ocean primary production sustained by rivers and coastal erosion. *Nat. Commun.* 12, 169 (2021).
- Ogorodov, S., Aleksyutina, D., Baranskaya, A., Shabanova, N. & Shilova, O. Coastal erosion of the Russian Arctic: an overview. J. Coast. Res. 95, 599–604 (2020).
- Guégan, E. Erosion of Permafrost Affected Coasts: Rates, Mechanisms and Modelling. PhD thesis, Norwegian Univ. Science and Technology (2015).
- Jones, B. M. et al. Increase in the rate and uniformity of coastline erosion in Arctic Alaska. Geophys. Res. Lett. 36, L03503 (2009).
- 184. Hasholt, B., van As, D., Mikkelsen, A. B., Mernild, S. H. & Yde, J. C. Observed sediment and solute transport from the Kangerlussuaq sector of the Greenland Ice Sheet (2006–2016). Arct. Antarct. Alp. Res. https://doi.org/10.1080/15230430.2018.1433789 (2018).
- Hudson, B. et al. MODIS observed increase in duration and spatial extent of sediment plumes in Greenland fjords. Cryosphere 8, 1161–1176 (2014).
- Overeem, I., Nienhuis, J. H. & Piliouras, A. Ice-dominated Arctic deltas. Nat. Rev. Earth Environ. https://doi.org/10.1038/s43017-022-00268-x (2022).
- Fritz, M., Vonk, J. E. & Lantuit, H. Collapsing Arctic coastlines. Nat. Clim. Change 7, 6–7 (2017).
- Huss, M. et al. Toward mountains without permanent snow and ice. Earths Future 5, 418–435 (2017).
- Schaefer, K., Zhang, T., Bruhwiler, L. & Barrett, A. P. Amount and timing of permafrost carbon release in response to climate warming. Tellus B 63, 165–180 (2011).
- Sadai, S., Condron, A., DeConto, R. & Pollard, D. Future climate response to Antarctic ice sheet melt caused by anthropogenic warming. Sci. Adv. 6, eaaz1169 (2020).

- Aschwanden, A. et al. Contribution of the Greenland ice sheet to sea level over the next millennium. Sci. Adv. 5, eaav9396 (2019).
- Knight, J. & Harrison, S. Mountain glacial and paraglacial environments under global climate change: lessons from the past, future directions and policy implications. Geogr. Ann. Ser. A 96, 245–264 (2014).
- Costa, A. et al. Temperature signal in suspended sediment export from an alpine catchment. Hydrol. Earth Syst. Sci. 22, 509–528 (2018).
- Church, M. & Slaymaker, O. Disequilibrium of Holocene sediment yield in glaciated British Columbia. Nature 337, 452–454 (1989).
- 195. Slosson, J. R., Kelleher, C. & Hoke, G. D. Contrasting impacts of a hotter and drier future on streamflow and catchment scale sediment flux in the High Andes. J. Geophys. Res. Earth Surf. https://doi.org/10.1029/2021if006182 (2021).
- Walling, D. E. Human impact on land-ocean sediment transfer by the world's rivers. Geomorphology 79, 192-216 (2006).
- Li, L. et al. Global trends in water and sediment fluxes of the world's large rivers. Sci. Bull. 65, 62–69 (2020).
- 198. Pandey, A., Himanshu, S. K., Mishra, S. K. & Singh, V. P. Physically based soil erosion and sediment yield models revisited. *Catena* **147**, 595–620 (2016).
- de Vente, J. et al. Predicting soil erosion and sediment yield at regional scales: where do we stand. Earth Sci. Rev. 127. 16–29 (2013).
- 200. Walling, D. E. The sediment delivery problem. J. Hydrol. 65, 209-237 (1983).
- Vercruysse, K., Grabowski, R. C. & Rickson, R. J. Suspended sediment transport dynamics in rivers: multi-scale drivers of temporal variation. *Earth Sci. Rev.* 166, 38–52 (2017).
- 202. Harrison, S. et al. Uncertainty in geomorphological responses to climate change *Clim. Change* **156**, 69–86 (2019).
- Qin, D. & Ding, Y. Key issues on cryospheric changes, trends and their impacts. Adv. Clim. Change Res. 1, 1–10 (2010).
- 204. Thackeray, C. W. & Hall, A. An emergent constraint on future Arctic sea-ice albedo feedback. *Nat. Clim. Change* **9**, 972–978 (2019).
- Fang, H.-W. & Wang, G.-Q. Three-dimensional mathematical model of suspendedsediment transport. J. Hydraul. Eng. 126, 578–592 (2000).
- Syvitski, James, P. M. & Milliman, J. D. Geology, geography, and humans battle for dominance over the delivery of fluvial sediment to the coastal ocean. J. Geol. 115, 1–19 (2007).
- Koppes, M. N. & Montgomery, D. R. The relative efficacy of fluvial and glacial erosion over modern to orogenic timescales. *Nat. Geosci.* 2, 644–647 (2009).
- 208. Hinderer, M., Kastowski, M., Kamelger, A., Bartolini, C. & Schlunegger, F. River loads and modern denudation of the Alps a review. *Earth Sci. Rev.* **118**, 11–44 (2013).
- 209. Wolman, M. G. & Miller, J. P. Magnitude and frequency of forces in geomorphic processes. *J. Geol.* **68**, 54–74 (1960).
- Gariano, S. L. & Guzzetti, F. Landslides in a changing climate. Earth Sci. Rev. 162, 227–252 (2016).
- McMillan, S. K. et al. Before the storm: antecedent conditions as regulators of hydrologic and biogeochemical response to extreme climate events. *Biogeochemistry* 141, 487–501 (2018).
- Schumm, S. A. Geomorphic thresholds: the concept and its applications. Trans. Inst. Br. Geogr. 4, 485–515 (1979).
- Phillips, J. D. Evolutionary geomorphology: thresholds and nonlinearity in landform response to environmental change. *Hydrol. Earth Syst. Sci.* 10, 731-742 (2006).
- Katzenberger, A., Schewe, J., Pongratz, J. & Levermann, A. Robust increase of Indian monsoon rainfall and its variability under future warming in CMIP6 models. *Earth Syst. Dyn.* 12, 367–386 (2021).
- Rao, M. P. et al. Seven centuries of reconstructed Brahmaputra River discharge demonstrate underestimated high discharge and flood hazard frequency. *Nat. Commun.* 11, 6017 (2020).
- Heckmann, T. et al. Indices of sediment connectivity: opportunities, challenges and limitations. Earth Sci. Rev. 187, 77-108 (2018).
- Syvitski, J. P. M., Vörösmarty, C. J., Kettner, A. J. & Green, P. Impact of humans on the flux of terrestrial sediment to the global coastal ocean. Science 308, 376 (2005).
- Piliouras, A. & Rowland, J. C. Arctic river delta morphologic variability and implications for riverine fluxes to the coast. J. Geophys. Res. Earth Surf. https://doi.org/10.1029/ 2019jf005250 (2020).
- Valenza, J. M., Edmonds, D. A., Hwang, T. & Roy, S. Downstream changes in river avulsion style are related to channel morphology. Nat. Commun. 11, 2116 (2020).
- $220.\ \ Liu, K.\ et\ al.\ Ongoing\ drainage\ reorganization\ driven\ by\ rapid\ lake\ growths\ on\ the\ Tibetan\ Plateau.\ Geophys.\ Res.\ Lett.\ https://doi.org/10.1029/2021gl095795\ (2021).$
- 221. Richardson, P. W., Perron, J. T. & Schurr, N. D. Influences of climate and life on hillslope sediment transport. Geology 47, 423–426 (2019).
- Zhou, Y. et al. Distinguishing the multiple controls on the decreased sediment flux in the Jialing River basin of the Yangtze River, southwestern China. Catena https://doi.org/ 10.1016/i.catena.2020.104593 (2020).
- Zhang, S., Fan, W., Li, Y. & Yi, Y. The influence of changes in land use and landscape patterns on soil erosion in a watershed. Sci. Total Environ. 574, 34-45 (2017).
- 224. Zhu, Z. et al. Greening of the Earth and its drivers. Nat. Clim. Change 6, 791–795 (2016).
- 225. Miao, C., Ni, J., Borthwick, A. G. L. & Yang, L. A preliminary estimate of human and natural contributions to the changes in water discharge and sediment load in the Yellow River. Glob. Planet. Change 76, 196–205 (2011).
- 226. Mouyen, M. et al. Assessing modern river sediment discharge to the ocean using satellite gravimetry. *Nat. Commun.* **9**, 3384 (2018).

- 227. Dethier, E. N., Renshaw, C. E. & Magilligan, F. J. Rapid changes to global river suspended sediment flux by humans. Science 376, 1447–1452 (2022).
- Huntley, D. et al. Field testing innovative differential geospatial and photogrammetric monitoring technologies in mountainous terrain near Ashcroft, British Columbia, Canada. J. Mt Sci. 18, 1–20 (2021).
- Piret, L. et al. High-resolution fjord sediment record of a receding glacier with growing intermediate proglacial lake (Steffen Fjord, Chilean Patagonia). Earth Surf. Process. Landforms 46, 239–251 (2020).
- 230. Deino, A. L. et al. Chronostratigraphic model of a high-resolution drill core record of the past million years from the Koora Basin, south Kenya Rift: overcoming the difficulties of variable sedimentation rate and higheses. *Quat. Sci. Rev.* 215, 213–231 (2019).
- Cook, K. L. et al. Detection and potential early warning of catastrophic flow events with regional seismic networks. Science 374, 87–92 (2021).
- Cohen, S., Kettner, A. J., Syvitski, J. P. M. & Fekete, B. M. WBMsed, a distributed globalscale riverine sediment flux model: model description and validation. Comput. Geosci. 53, 80–93 (2013).
- Kettner, A. J. & Syvitski, J. P. M. HydroTrend v.3.0: a climate-driven hydrological transport model that simulates discharge and sediment load leaving a river system. Comput. Geosci. 34, 1170–1183 (2008).
- Nearing, M. A., Foster, G. R., Lane, L. & Finkner, S. A process-based soil erosion model for USDA-Water Erosion Prediction Project technology. *Trans. ASAE* 32, 1587–1593 (1989).
- Reichstein, M. et al. Deep learning and process understanding for data-driven Earth system science. Nature 566, 195–204 (2019).
- Huang, L., Luo, J., Lin, Z., Niu, F. & Liu, L. Using deep learning to map retrogressive thaw slumps in the Beiluhe region (Tibetan Plateau) from CubeSat images. Remote Sens. Environ. https://doi.org/10.1016/j.rse.2019.111534 (2020).
- Tan, Z., Leung, L. R., Li, H. Y. & Tesfa, T. Modeling sediment yield in land surface and Earth System models: model comparison, development, and evaluation. J. Adv. Model. Earth Syst. 10, 2192–2213 (2018).
- Pfeffer, W. T. et al. The Randolph Glacier inventory: a globally complete inventory of glaciers. J. Glaciol. 60, 537–552 (2014).
- 239. Obu, J. et al. ESA Permafrost Climate Change Initiative (Permafrost\_cci): Permafrost active layer thickness for the Northern Hemisphere, v3.0 (NERC EDS Centre for Environmental Data Analysis, 2021); https://catalogue.ceda.ac.uk/uuid/67a3f8c8dc914ef99f7f08eb0d997e23
- Strauss, J. et al. Database of ice-rich Yedoma permafrost (IRYP). PANGAEA https://doi.org/ 10.1594/PANGAEA.861733 (2016).

#### **Acknowledgements**

This work was supported by Singapore MOE (A-0003626-00-00; D.L., X.L.), the Intergovernmental Panel on Climate Change and the Cuomo Foundation (D.L.). The authors acknowledge comments provided by M. Church. We thank O. Jaroslav, R. MacLeod, J. Comte, L. Huang and W. Pollard for providing field photos. Any use of trade, firm or product names is for descriptive purposes only and does not imply endorsement by the US Government.

#### **Author contributions**

T.Z. and D.L. conceived the study and assembled the authorship team. T.Z. and D.L. drafted the paper. All authors contributed to the discussion and editing of the manuscript prior to submission.

#### **Competing interests**

The authors declare no competing interests.

#### **Additional information**

Supplementary information The online version contains supplementary material available at https://doi.org/10.1038/s43017-022-00362-0.

Correspondence should be addressed to Dongfeng Li.

Peer review information Nature Reviews Earth & Environment thanks Greta Wells, Joel Rowland and the other, anonymous, reviewer(s) for their contribution to the peer review of this work

Reprints and permissions information is available at www.nature.com/reprints.

**Publisher's note** Springer Nature remains neutral with regard to jurisdictional claims in published maps and institutional affiliations.

Springer Nature or its licensor (e.g. a society or other partner) holds exclusive rights to this article under a publishing agreement with the author(s) or other rightsholder(s); author self-archiving of the accepted manuscript version of this article is solely governed by the terms of such publishing agreement and applicable law.

© Springer Nature Limited 2022